OVERVIEW OF CRETACEOUS OCEANIC RED BEDS (CORBs): A WINDOW ON GLOBAL OCEANIC AND CLIMATE CHANGE

CHENGSHAN WANG
Geological Centre of the Tibetan Plateau, China University of Geosciences, Beijing 100083, P.R. China
e-mail: chshwang@cugb.edu.cn
XIUMIAN HU
State Key Laboratory of Mineral Deposit Research, Department of Earth Sciences, Nanjing University, Nanjing 210093, P.R. China
e-mail: huxm@nju.edu.cn
YONGJIANG HUANG
Geological Centre of the Tibetan Plateau, China University of Geosciences, Beijing 100083, P.R. China
e-mail: huangyj@cugb.edu.cn
ROBERT W. SCOTT
Precision Stratigraphy Associates and University of Tulsa, 149 West Ridge Road, RR3 Box 103-3, Cleveland Oklahoma 74020, U.S.A.
e-mail: rwscott@ix.netcom.com
AND
MICHAEL WAGREICH
University of Vienna, Department of Geodynamics and Sedimentology, Althanstraße 14, A-1090 Vienna, Austria
e-mail: michael.wagreich@univie.ac.at

Abstract: Cretaceous oceanic red beds (CORBs) are mainly pelagic red shales, marls, or fine-grained limestones. These facies have been the subject of two closely related International Geosciences Programs GCP 463 and 494. They are a significant facies of deep-water pelagic deposits and pelagic–hemipelagic sedimentary systems. A major contribution of these two three- and five-year projects is that CORBs are globally distributed in outcrops in Europe, Asia, Africa, New Zealand, Caribbean, and at DSDP and ODP sites in the Tethyan Atlantic, Pacific, and Indian oceans. CORBs experienced two paleogeographical expansions, (1) in Aptian nannofossil zone CC7 shortly after the OAE1a and (2) in Turonian zone CC11 after the OAE2, respectively. Lower Cretaceous CORBs are much less common than Upper Cretaceous. Above OAE2, CORBs in zone CC11 crop out in 25 basins or tectonic zones; CORB distribution is greatest in Coniacian–Early Santonian zones CC13–CC15 in up to 34 basins or tectonic zones in the world.

The ages of CORBs are constrained by paleontological data including planktic foraminifera and nannofossils in calcareous CORBs, and agglutinated foraminifera and dinoflagellates or radiolaria in noncalcareous CORBs. The biostratigraphic data were assembled into an integrated, testable data base by graphic correlation. The data base was then correlated to GSSPs and reference sections of Cretaceous stages.

Three general facies types of CORB are defined using the end members clay, carbonate, and chert: deep-water red claystones deposited below the calcite compensation depth, red hemipelagic and pelagic carbonates, and red cherts and radiolarites. The depositional environment of most CORB units was in relatively deep oceanic basins. Deposition was generally far from shoreline and only locally associated with coarse terrigenous clastics such as turbidites. Significant controlling factors of CORBs were slow sediment accumulation rates at great paleo–water depths. Like most marine sediments, CORBs are a complex mixture of terrigenous detritus and seawater-derived material.

According to data reported from the studied localities, the common geochemical properties of CORBs are their extremely low organic-carbon content and high level of ferric oxides. The ratio between ferric oxides to the total iron is not only higher than the level of adjacent non-red sediments, but also higher than that of Phanerozoic normal marine oxic sedimentary rocks. These chemical properties indicate that CORBs were deposited in environments that were highly oxic at or below the sediment–water interface. Other major and trace elements and isotopic data suggest an oxic, oligotrophic water mass having overall low productivity. The paleoceanographic and paleoclimatological conditions are corroborated by carbon stable-isotope data, phosphorus burial records, dissolved-oxygen index, and comprehensive geochemical modeling results. Paleoclimate, paleogeography, ocean currents, and nutrient flux, among other processes, were related to the deposition and wide distribution of CORBs during the Late Cretaceous. The development of the paleogeographic configuration and Late Cretaceous climate cooling provided the basis for increasing ventilation of the deep ocean. The behavior of redox-sensitive nutrient elements like phosphorus further stimulated the development of oligotrophic conditions. All of these factors contributed to the global distribution of CORBs.

Key words: Cretaceous oceanic red beds, sedimentology, mineralogy, geochemistry, geographic distribution, stratigraphic distribution, biostratigraphy, paleoclimate, paleoceanography

Cretaceous Oceanic Red Beds: Stratigraphy, Composition, Origins, and Paleoceanographic and Paleoclimatic Significance
SEPM Special Publication No. 91, Copyright © 2009
SEPM (Society for Sedimentary Geology), ISBN 978-1-56576-135-3, p. 13–33.

INTRODUCTION

CORBs are red to pink to brown, fine-grained sedimentary rocks of Cretaceous age deposited in pelagic marine environments. Red radiolarian cherts interbedded with argillic or carbonate red beds are included. This definition of oceanic red beds does not include red sediments that were derived from erosion of continental red beds (Van Houten, 1964) and transported from continental to marine environments. Upper Cretaceous pelagic "red" or "multicolored," noncalcareous clays were first cored in the western North Atlantic (Arthur, 1979). These beds overlie organic-rich black shale, which Arthur suggested was the source of ferrous iron that diffused up into the slowly accumulating oxygen-rich clay. Since then, however, these red marine clays have not received intensive, coordinated study. We hope that this volume will address this research gap.

From 2002 to 2006 CORBs have been the scientific topic of two closely related International Geosciences Programs, IGCP 463 "Upper Cretaceous Oceanic Red Beds: Response to Ocean/Climate Global Change" (2002–2006) and IGCP 494 "Dysoxic to Oxic Change in Ocean Sedimentation During Middle Cretaceous: a Study of the Tethyan Realm" (Young Scientists Project, 2003–2005). The objective of IGCP 463 was to study major paleoceanographic phenomena recorded by sedimentary sequences in the world's oceans. CORBs followed widespread deposition of mid-Cretaceous organic-carbon-enriched shales characterized by deposition in a dysoxic to anoxic deep ocean environment. The depositional change in the Late Cretaceous was to reddish clays and marls in oxic marine conditions. The aim of the Young Scientist Project IGCP 494 was to gain knowledge about the mid-Cretaceous oceanographic conditions that caused occasional changes from dysoxic–anoxic to oxic deep-sea sedimentation.

To achieve these goals during the past five years over 100 scientists from more than 20 countries actively engaged in the projects. Eight international workshops, sessions, and field trips were organized in Ancona, Italy (2002), Bartin, Turkey (2003), Bremen, Germany (2003), Bucharest, Romania (2004), Florence, Italy (32IGC, 2004), Vienna, Austria (EGU, 2005), Neuchatel, Switzerland (7th ISC, 2005), and Beijing, China (2006). Participants were mainly devoted to: (1) investigating the occurrences, distributions, lithologies, ages, and depositional environments of the CORBs; (2) establishing reference sections in many areas around the world, such as central Italy, Austria, southern Tibet, Romania, Poland, Turkey, and ODP cores (such as ODP 1049) in the Atlantic Ocean for more detailed studies; and (3) investigating a broad range of methods and techniques including stratigraphy, sedimentology, paleontology, geochemistry, and stable isotopes to understand the nature of the CORBs.

A number of publications, including many scientific peer-reviewed papers, field guides, and meeting abstracts, were published in both international and regional journals. Papers were published in two special volumes on the topic of CORBs, one in *Cretaceous Research* (2005, Volume 26, Issue 1) and another in *Earth Science Frontiers* (2005, Volume 12, Issue 2). This SEPM Special Publication on the topic of Cretaceous oceanic red beds will collect comprehensive studies on CORBs from different areas using different methods and is the main report for IGCP 463 and 494.

TEMPORAL–SPATIAL DISTRIBUTION OF CORBs

A major achievement of IGCP 463 and 494 is that they provide evidence that CORBs are globally distributed, including outcrops in Europe, Asia, Africa, New Zealand, the Caribbean, and cores at DSDP and ODP sites in the Tethyan Atlantic, Pacific, and Indian oceans (Fig. 1, Appendix 1; Hu et al., 2005; Hu et al., 2006a).

The initial chronostratigraphic framework for the study of CORBs was the nannofossil zonal scheme of Sissingh (in Perch-Nielsen, 1985). These zones have been calibrated to numerical ages by Ogg et al. (2004). The more up-to-date zonation of Burnett (1998) was not used because most of the biostratigraphic data acquired during the project used the 1985 zones. However, project stratigraphers recognized that the Perch-Nielsen (1985) zonation scheme has some inconsistencies, especially in the Turonian–Santonian. For the tally of Figure 2, all sections having a CORB interval within one CC zone were counted as 1. Each basin or tectonic zone was counted as 1.

Continental CORB Occurrences

Lower Cretaceous (CC1–CC6) CORBs are known from only Berriasian–Barremian outcrops in only three places (Figs. 1A, 2A). The Valanginian to lowermost Hauterivian red shales in Greenland are only a few meters thick (Alsen and Surlyk, 2004). The Upper Berriasian to Lower Valanginian CORBs in the Northern Calcareous Alps, Austria, are about 5 m thick and consist of marly limestones and marls (Wagreich, this volume). About 7 meters of pale red to reddish-gray pseudo-nodular limestone were cored in the CISMON APTICORE, northern Italy (Erba et al., 1999) in zone CC5. Therefore, CORBs were deposited rarely in Early Cretaceous in very local areas. However, if we include the special facies type of red cherts, radiolarites, and radiolarite–shale cyclic successions associated with ophiolite suture zones, such as the Lower Cretaceous red cherts and radiolarites in the Indus–Yarlung Zangbo Suture Zone (Ziabrev et al., 2003) and in the Pindos Basin of Greece (Neumann and Wagreich, this volume), such siliceous CORBs were more widespread in oceanic settings.

Mid-Cretaceous (CC7–CC10) Aptian–Cenomanian CORB outcrops are well exposed in the Umbria-–Marche Basin of central Italy (site 24 in Figs. 1B, 2A, Appendix 1), as well as in the Southern Alps (site 26), the Austrian Alps (sites 5, 6, 7), the Czech Republic (sites 11, 13), Albania (site 2), Germany (sites 16, 17), New Zealand (site 27), the Carpathians of Poland and Slovakia (site 28), Romania (site 33), Spain (site 38), Switzerland (site 39), Turkey (site 40), the northern Caucasus (site 44), northeastern England (site 50), as well as in the Zanskar Himalayas (site 22) and California, U.S.A. (site 47, Fig. 1B) (see Appendix 1). After the OAE1a Selli Level, CORBs deposition became more widespread geographically from 3 basins or tectonic zones in zone CC7, to 7 basins or tectonic zones in zone CC8, and to 12 basins–tectonic zones in zones CC9 and CC10 (Fig. 2A).

Mid-Cretaceous CORBs commonly occur as discrete thin beds. For example, in the Umbria–Marche basin eight reddish-colored intervals (named as ORB1 to ORB8) are embedded in mid-Cretaceous sedimentary strata (Hu et al., 2006a). The oldest is of Aptian age, located just above the Selli Level, and the youngest is middle Cenomanian. The age span of each red-bed interval is relatively short, with the longest being the one above Selli (ORB1), lasting about 4.54 Myr, and the shortest (ORB4) in the middle Albian, with a time span of only about 0.13 Myr (Hu et al., 2006a).

Upper Cretaceous (CC11–26) Turonian to Maastrichtian CORBs were deposited mainly in the Tethys sea and are now exposed in Tibet, India, Europe, the Caribbean, and New Zealand (Figs. 1C, 2A). CORB deposition resumed soon after the end of OAE2 Bonarelli Level and experienced the second geographic expansion in the Middle–Late Turonian (CC11). Among CC11–CC19 Turonian–Lower Campanian CORBs occur in more than 20

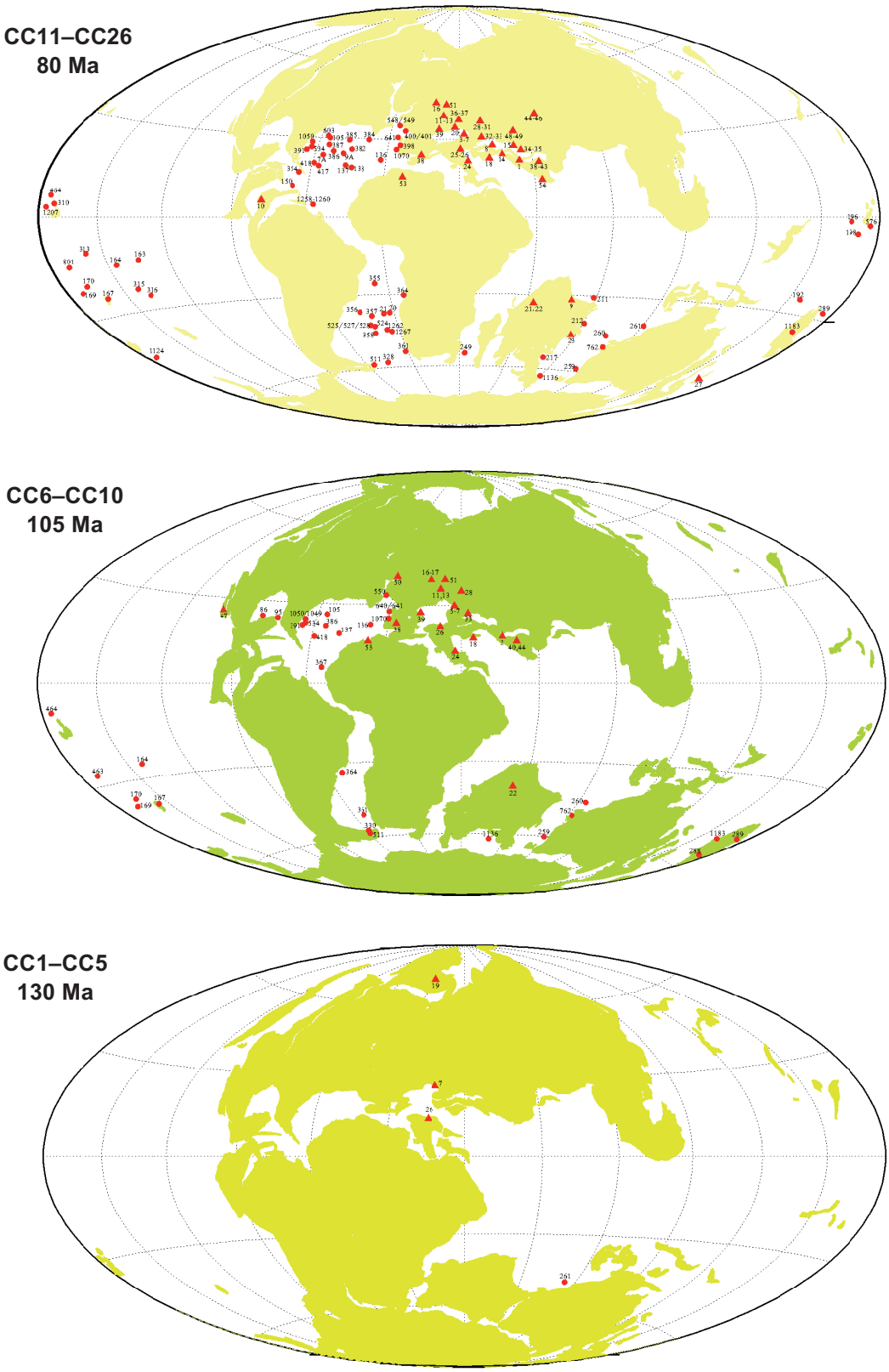

FIG. 1.—Paleogeographic map showing the localities of CORBs both on continents and in oceans. **A)** Early Cretaceous (85 Ma); **B)** Mid-Cretaceous (105 Ma); **C)** Late Cretaceous (130 Ma). The paleogeographic base maps are from Hay et al. (1999), downloaded from the website www.odsn.de

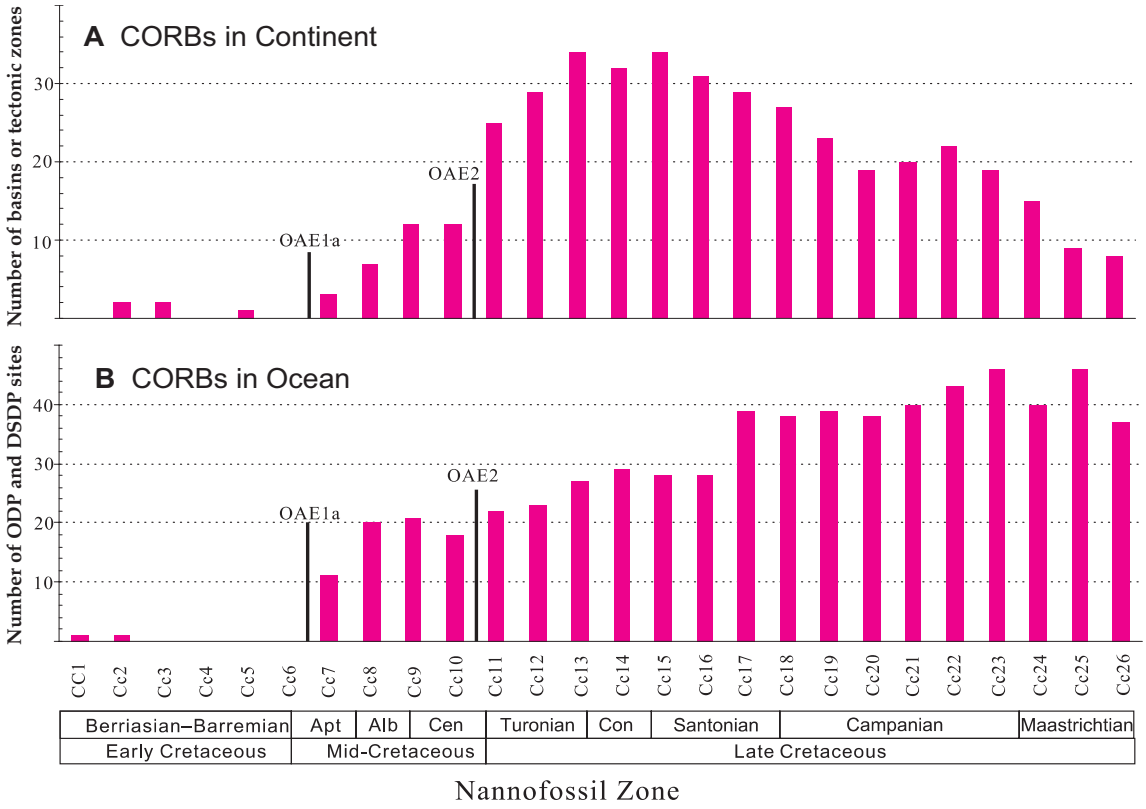

FIG. 2.—Nannofossil-zone distribution of CORBs based on a global survey of **A)** 53 basins or tectonic zones discovered in continents, and **B)** 75 DSDP and ODP sites from oceans.

basins or tectonic zones, and are most widespread and common in global deep-sea basins. However, during the Late Cretaceous CORBs were not deposited in some shallower epicontinental basins in the North American Western Interior or in the marginal basins of Colombia and Venezuela, or in the Neuquen Basin of Argentina. They are also absent in African epicontinental basins. But they are present in the European epicontinental chalk basin, such as red limestones in Germany (e.g., Wiese, this volume) and red chalk in England (Mitchell, 1995). Late Campanian–Maastrichtian (CC20–26) CORBs are less widespread comparing to Turonian-Early Campanian widely distribution. CORBs locally are overlain by Danian pelagic red beds, as in central Italy and southern Spain (Hu et al., 2005), in the Romanian Carpathian Mountains (Bojar et al., this volume; Melinte, this volume) and in the North Atlantic (Scott, this volume) among other places. So the oceanic processes that produced red pelagic, fine-grained sediments were not terminated by the end-Cretaceous crisis. However, at any one place CORB deposition was not continuous because of local basinal tectonic and paleogeographic conditions. Based on continental sections, CC13–CC15 (Coniacian–Early Santonian) was the maximum time of CORB deposition (Fig. 2A). Shallow-water red limestones occur in northwestern Germany (CC10–14 or 15), Jordan (CC11), North Africa, and Tunisia (CC10–13) (Wiese, this volume; Jens Wendler et al., this volume).

Oceanic CORB Occurrences

The CORBs recovered from the DSDP and ODP sites are located mainly in four regions of the global ocean: the North Atlantic in low to mid latitudes of the northern hemisphere, the South Atlantic and the Indian Ocean in the mid to high latitude of the southern hemisphere, and the central Pacific Ocean (Chen et al., 2007) (see Appendix 2). Each DSDP or ODP site was counted as 1 for the tally (Fig. 2), not like basin or tectonic zone used in continental data. Therefore, we consider that the CORB distribution in DSDP and ODP sites may not be accurate because certain areas may have many DSDP and ODP Cretaceous sites such as the northern Atlantic, whereas some areas may have no or very few drilling sites such as large areas of the Pacific.

Early Cretaceous (CC1–CC6) (Fig. 2B) CORBs are identified only from site DSDP 261 in the eastern Wharton Basin of the eastern Indian Ocean. The sediments are Berriasian–Valanginian (CC1–2) in age and consist mainly of semilithified brown claystones. The CORBs of this age are sporadically distributed in the deep-water oceans, which indicates that the occurrence of CORBs is local and has little implications for the global ocean.

Mid-Cretaceous (CC7–CC10) CORB deposition began during Aptian zone CC7 and became widespread in the global ocean from then on (Figs. 1B, 2B). After zone CC7, red or brown sediments (mainly clays, marls, and limestones) were deposited at 11 to 21 sites during any one or more of these younger nannofossil zones. Consequently CC7 is thought to mark the onset of global CORB deposition, similar to data documented in continental outcrops.

Late Cretaceous CORB deposition (CC11–26) began during Turonian zone CC11 (Figs. 1A, 2B). CORBs are recorded at 20–40 sites and in every nannofossil zone from CC11 to CC16. The most widespread CORB deposition was in latest Santonian zone CC17 to Maastrichtian zone CC26. CORBs have been recovered from more than 40 sites in zones CC21–CC25.

BIOSTRATIGRAPHY AND PALEOECOLOGY

Oceanic red beds identified during projects IGCP 463 and 494 span the Aptian to Maastrichtian stages (Bak, 2002; Melinte and Jipa, 2005; Hu et al., 2005; Wagreich et al., this volume) (Fig. 3), although locally marine red beds are Berriasian–Valanginian. IGCP 463 and 494 participants prepared biostratigraphic check lists that were the basis of both zonal definitions and graphic correlation experiments. In calcareous CORBs planktic foraminifera and nannofossils were the most reliable dating criteria. In argillaceous CORBs benthic agglutinated foraminifera were the principal age criterion. In some sections dinoflagellates or radiolaria were also identified. Megafossils generally were absent, but in some sections inoceramid shells, ammonites, belemnites, and echinoids were very rare. Inoceramids were adapted to a benthic habitat in low-oxygen bottom waters (MacLeod and Hoppe, 1992). Abyssal inoceramids became extinct during the mid-Maastrichtian as cool bottom waters became well oxygenated (MacLeod et al., 1996). So the absence of these bivalves in CORBs may be negative evidence supporting the oxygen-rich conditions of CORBs.

Two approaches were taken to interpolate numerical ages on the bases and tops of marine red beds. The bases and tops of biozones have been interpolated into the recently revised Cretaceous time scales (Hardenbol and Robaszynski, 1998; Ogg et al., 2004). Biozones of planktic foraminifera, calcareous nannoplankton, and benthic agglutinated foraminifera are present in many CORBs. A second method to interpolate ages was by graphic correlation of selected CORB sections with the MIDK42 chronostratigraphic database (Scott, this volume). This database was calibrated first to the 1989 time scale (Harland et al., 1990) and subsequently to the revised 2004 scale (Ogg et al., 2004). The differences in ages between these two approaches are generally small (see discussion by Scott, this volume). An important question, however, is whether the species ranges in each section correlate with the maximum known ranges. The zonal method cannot test this hypothesis, whereas the graphic correlation method does. Graphic correlation hypotheses can be evaluated and tested by nonbiostratigraphic data. The two methods result in comparable age ranges, although graphic correlation generates more precise ages.

Planktic foraminifera in marine red beds and associated lithologies define standard Upper Cretaceous zones. Among other locales, they are reported in the North Atlantic DSDP 382, 385, and 398, in Tibet (Wan et al., 2005), and in the Southern Cauvery

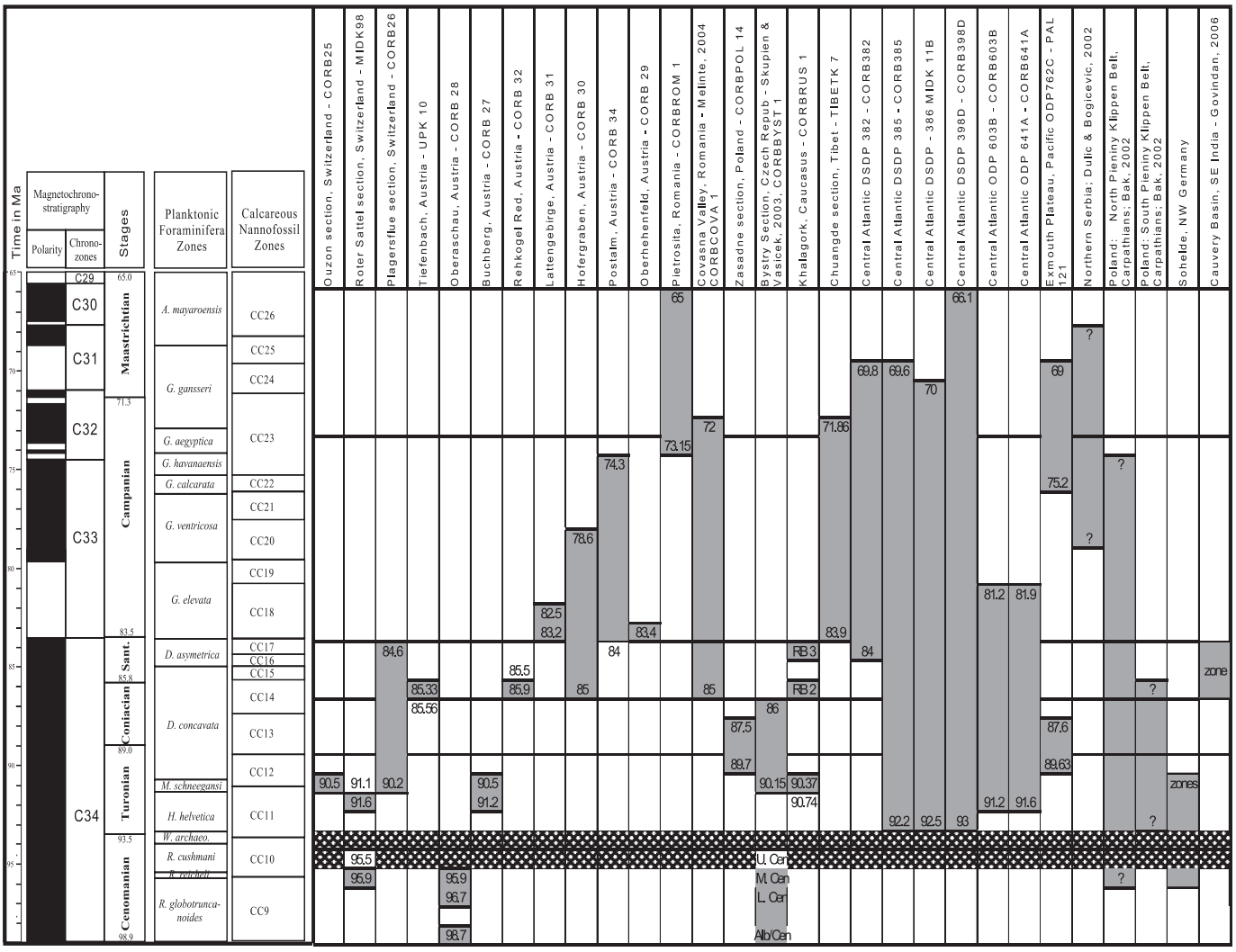

FIG. 3.—Ages of CORB sections in study measured by graphic correlation plotted on the Ogg et al. (2004) time scale.

Basin, India. In the Bottaccione Gorge section, reddish carbonates comprise Turonian–Maastrichtian planktic foraminifera zones (Hu et al., 2006a; Hu et al. this volume). Planktic foraminifera occur together with inoceramids in the Santonian of Austria and in the Turonian–Coniacian of New Zealand (Hikuora et al., this volume). Planktic foraminifera indicate normal marine conditions. Their absence in CORBs indicates that deposition was below the CCD.

Benthic foraminifera are present in nearly all CORBs both on land and in oceanic cores. In some basins agglutinated benthic foraminifera are the only age criterion. Three of the four agglutinated benthic foraminifera zones are defined in the sections studied: *Uvigerinammina jankoi* Majzon, *Caudammina gigantea* Geroch (also in *Hormosina*), and *Goesella rugosa* (Hanzlikova). New data reported by Skupien et al. (this volume) suggest that some ranges will be modified. The Late Cretaceous agglutinated benthic foraminifera *Haplophragmoides, Glomospira, Karrerulina, Praecystammina*, and *Uvigerinammina* are diagnostic of the abyssal depth zone (Kuhnt et al., 1996). Because these agglutinated foraminifera live in the uppermost few centimeters below the sediment–water interface (Kuhnt et al., 1996), their presence indicates oligotrophic oxic bottom conditions during red-bed deposition. Changes in benthic foraminiferal assemblages from the onset of CORB sedimentation in Early to Middle Turonian indicate stepwise changes from dysoxic to oxic bottom water conditions (Ines Wendler et al., this volume).

Nannofossils are recovered in most calcareous CORB strata. Turonian to Maastrichtian CORBs and intervening mud rocks in Austria and Romania yield species of the calcareous nannofossil zones CC11 to CC26 (Wagreich, this volume; Melinte et al., this volume, Bojar et al., this volume; zonation of Sissingh, 1977). In the North Atlantic DSDP 398, 385, and 382 cores they are also common. In the Bottaccione Gorge section reddish carbonates include Turonian–Maastrichtian nannofossil zones CC11 or CC12 to NC23 (Hu et al., 2006a).

Dinoflagellates are important in CORBs and associated deposits in the Carpathians of the Czech Republic (Skupien et al., this volume) and in the North Atlantic DSDP 603 and ODP 641 cores. In Austrian CORB facies dinoflagellates occur with planktic foraminifera and nannofossils and integrate zones of each group (Wagreich et al., 2006). With closely spaced sampling and processing they probably will be discovered in other CORB sections. Dinoflagellate assemblages are a clue to distinguish between oligotrophic and eutrophic oceanic water masses. In the central Atlantic at ODP 641A, dinoflagellate diversity decreases from the Albian–Cenomanian into the Cenomanian–Turonian black clay of OAE2, which yielded five species (Thurow et al., 1988). Twelve species are present in the green clay of the recovery interval above the black clay, but the overlying brown clay of the CORB is barren of dinoflagellates, which may be the result of oxidation of organic matter in the water column. The black clay of OAE2 was deposited between 93.53 Ma and 93.07 Ma in the MIDK42 chronostratigraphic database. The overlying green clay may represent a condensed interval, and CORB deposition began no later than 92.30 Ma based on the ages of the benthic foraminifera, a duration no greater than 670 kyr. Likewise, Turonian and Santonian CORBs in DSDP 603B are barren of dinoflagellates, but the intervening Coniacian green clays have diverse dinoflagellates (Habib and Drugg, 1987). However, basin-margin CORBs in the Turonian–Coniacian Silesian Unit of the Czech Republic yield only few species of dinoflagellates in low numbers (Skupien et al., this volume). This very small sample of CORB sections shows that study of dinoflagellates may be fruitful in testing marine productivity during CORB deposition.

Radiolaria are common in black shales at the Cenomanian–Turonian boundary but are rare in CORBs, although they have been reported in the North Atlantic DSDP 603, in the Pindos Basin of Greece (Neumann and Wagreich, this volume), and in Polish Carpathian sections spanning the Cenomanian–Turonian interval (Bak, 2002).

Trace fossils are rare in CORBs, but some beds host distinct burrow types such as *Thalassinoides*, *Planolites*, *Chondrites*, and *Zoophycus*. Most CORB deposits are homogeneous and not thinly laminated. This suggests that the sediments may have been bioturbated. Because of the lack of grain-size differentiation or composition, burrow mottling is not evident in many CORB outcrops. However, bioturbation is expected in oxic benthic environments.

MINERAL COMPOSITION

CORBs in the Chuangde Formation of southern Tibet are composed of nine red lithofacies (Hu et al., 2006b): (1) red foraminiferal packstone and grainstone, (2) red microfossil wackestone, (3) red marlstone with microfossils, (4) red marlstone, (5) red to variegated floatstone and rudstone (debris flow), (6) red shale, (7) red radiolarite, (8) red chert with radiolaria, and (9) red chert. The clay minerals in the gray beds of the Chuangde Formation are the same as those in other red beds, dominated by illite (65–90%) and chlorite (~ 30%). Based on XRD and diffuse reflectance spectrophotometry (DRS) data, Hu et al. (2006b) suggested that the red color is due to the presence of microscopic, finely dispersed hematite. The hematite could be synsedimentary or early diagenetic in origin.

The limestones of the Scaglia Rossa Formation in Italy are composed mainly of calcite (about 95% $CaCO_3$ on average) with minor clay minerals (mainly mixed-layer, illite–smectite, illite, and traces of kaolinite and chlorite) (Arthur and Fischer, 1977; Johnsson and Reynolds, 1986). Most reddish samples are characterized by the presence of illite, mixed-layer illite–smectite, kaolinite, and/or chlorite, but the relative proportions of these constituents vary widely. As compared to the limestone, shale partings are consistently enriched in mixed-layer illite–smectite, which is commonly more ordered and more illitic. Also, the limestones contain significant amounts of quartz in the clay size fraction but the shale partings do not. The mineral compositions of the shales differ qualitatively and quantitatively from those of the limestones. Johnsson and Reynolds (1986) concluded that the different proportions of clay fractions of the two lithologies resulted from cyclic climatic variability. Elsewhere Turonian marlstones and marly limestones in the transition from OAE2 black shales to CORBs in the Eastern Alps are composed of between 43% and 98% calcite; illite, chlorite, smectite, and low amounts of kaolinite are present in the clay size fraction (Neuhuber et al., 2007).

Hu et al. (this volume) present high-resolution mineralogical data of visible reflectance from the transition zone between the Scaglia Bianca Formation to the Scaglia Rossa Formation in the Vispi Quarry section, Umbria–Marche Basin, Italy. The data on diffuse reflectance spectrophotometry (DRS) show that the positive correlation between the peak height of hematite and redness values indicates that hematite concentration is responsible for the color of the limestones in the Vispi Quarry section. These authors concluded that the red color of the Scaglia Rossa limestones is the result of low concentration (~ 0.1 wt %) of finely dispersed hematite.

The magnetic properties of the Scaglia Rossa pelagic red beds vary depending on the type or iron mineral (Channell et al., 1982). The boundaries of paleomagnetic reversals defined by hematite

are a few tens of centimeters below those of magnetite. Thus, some of the hematite grains were magnetized in the post-reversal field, which demonstrates that growth of hematite crystals occurred with ~ 10^5 years during early diagenesis.

The mineral composition of cyclically interbedded red beds differs from that of greenish hemipelagic clayey nannofossil chalk. In the North Atlantic ODP 1050C Maastrichtian hemipelagic clayey chalk (~ 60–95% $CaCO_3$), the major minerals in the acid-insoluble residues of the < 63 μm fraction are quartz, clays (smectite, illite, kaolinite, and chlorite), and feldspars. The greenish intervals are enriched in kaolinite and feldspars, whereas in the reddish intervals quartz, illite, and chlorite are more abundant (Macleod et al., 2001). The clay size fraction (< 2 μm) has high amounts of smectite, illite, and kaolinite, and minor amounts of chlorite, quartz, and feldspars. However, the mineral composition of the different-colored beds displays no obvious cyclical variation in the clay size fraction.

SEDIMENTOLOGY AND DEPOSITIONAL ENVIRONMENTS

CORBs are red to pink to brown, fine-grained sedimentary rocks deposited in pelagic marine environments. The sedimentological parameter, fine grain size, is consistent with a pelagic, deeper marine depositional environment. Principally, CORBs constitute a special type of pelagic–hemipelagic deposits, distinguished from their gray counterparts only by their red or brownish color, and, consequently, they can be described and classified in the context of common classifications of deep-water pelagic deposits and pelagic–hemipelagic sedimentary systems (Fig. 4; e.g., Stow et al. 1996). CORBs were deposited by settling of particles through the water column and are mainly mixtures of terrigenous and biogenous components, as are gray-colored pelagic sediments. Red-colored turbidite mudstones are not included in this definition.

Case studies of CORBs indicate three general facies types: deep-water red claystones deposited below the calcite compensation depth, red hemipelagic and pelagic carbonates, and red cherts and radiolarites. A ternary classification (Fig. 4) is based on the end members clay, carbonate, and chert, which mimics general classifications of pelagic–hemipelagic deep-water sediments. Clayey CORBs, consisting mainly of clay minerals, are comparable to recent red (or brownish) pelagic clays; calcareous CORBs are mainly pelagic limestones like the Italian Scaglia Rossa; and siliceous CORBs consist mainly of biogenous SiO_2. Biogenous carbonate is mainly derived from calcareous nannofossils and planktic foraminifera; biogenous silica is mainly from radiolaria and, to a lesser degree, diatoms and sponge spiculae; and terrigenous clay and silt-size quartz is derived mainly from continental erosion and transported either by ocean currents or by wind. Cyclic CORBs are composed of interbedding of end members, e.g., red marl–limestone or chert–shale rhythmites.

Depositional environments of most CORBs were relatively deep-water in oceanic basins and at least pelagic in the sense that these environments are generally far away from shorelines and not associated with coarse terrigenous clastic facies (Fig. 5). Less commonly, relatively shallow but nevertheless offshore CORBs have been reported from epicontinental seaways in the chalk facies of Great Britain (Red Chalk; e.g., Mitchell, 1995) and Germany (Rotpläner; Wiese, this volume) and from distal carbonate platforms of Jordan (Jens Wendler et al., this volume). These were deposited below storm wave base in a few tens of meters water depths and far from respective coast lines. These CORBs display high carbonate contents and lower sediment accumulation rates than intercalated and associated gray or white facies types.

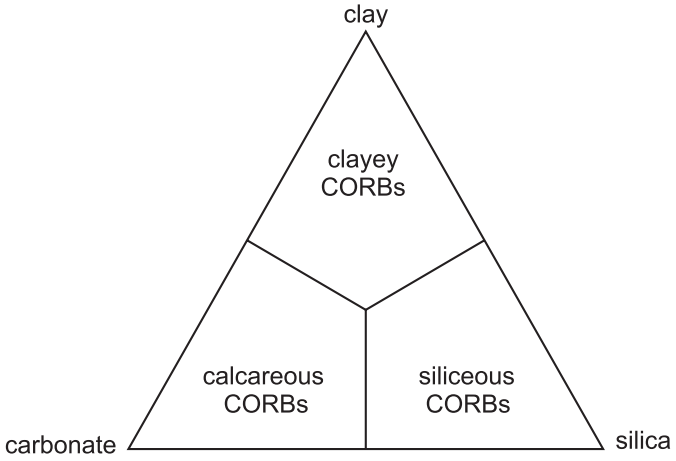

FIG. 4.—Classification of CORBs in the three-component pelagic–hemipelagic system according to Stow et al. (1996). Clay includes mainly terrigenous silt and clay, carbonate comprises mainly calcareous biogenic microfossils such as planktic foraminifera, calcareous nannofossils, and pteropod shells, and silica includes mainly biogenic silica of siliceous microfossils such as radiolaria and diatoms.

Outer-shelf to upper–middle bathyal CORBs comprise mainly red pelagic limestones characterized by high amounts of planktic foraminifera, and are a widespread facies type in low paleolatitudes, especially in the Tethyan paleogeographic realm (e.g., Spain, Italy, Austria, Greece, Turkey, Indian Himalaya). Examples from higher paleolatitudes (e.g., Greenland; Alsen and Surlyk, 2004; and New Zealand; Hikuroa et al., this volume) are relatively scarce. They have lower carbonate content and can be classified mainly as hemipelagic shales or marlstones. Outer-shelf to bathyal CORBs are commonly rhythmically bedded and comprise limestone–marl cycles driven by Milankovitch cyclicity, mainly precession (18 and 21 kyr) and obliquity (40 kyr) (Neuhuber et al., 2007). Cycles can be controlled by varying either terrigenous input or carbonate production due to changing climate.

Towards deeper bathyal depths, carbonate content decreases as the depositional area approaches the calcite lysocline. Red pelagic limestones and cyclic CORBs become scarce, and marls and marly shales become the dominant lithological facies type. Below the calcite compensation level, in abyssal depths, either red claystones and carbonate-free shales or cherts are deposited, depending on the proportion of terrigenous input. The sediment input is controlled largely by eolian transport or oceanic bottom currents, and siliceous biogenous production, which, compared to recent distributions of siliceous oozes, requires a high nutrient supply, as in oceanic upwelling regions today.

Slow sediment accumulation rates and great paleowater depth of the depositional area are significant controlling factors of CORBs. Several case studies indicate an increase in the number and thickness of CORB intervals along depositional gradients and within sections where paleo–water depth increased from neritic to bathyal depths. In the Austrian Helvetic shelf to slope margin setting, only decimeter-thick red intervals occur in outer-shelf micritic limestones, whereas the bathyal successions of the Ultrahelvetics are characterized by a continuous calcareous CORB interval during the same time interval. Transgressive succes-

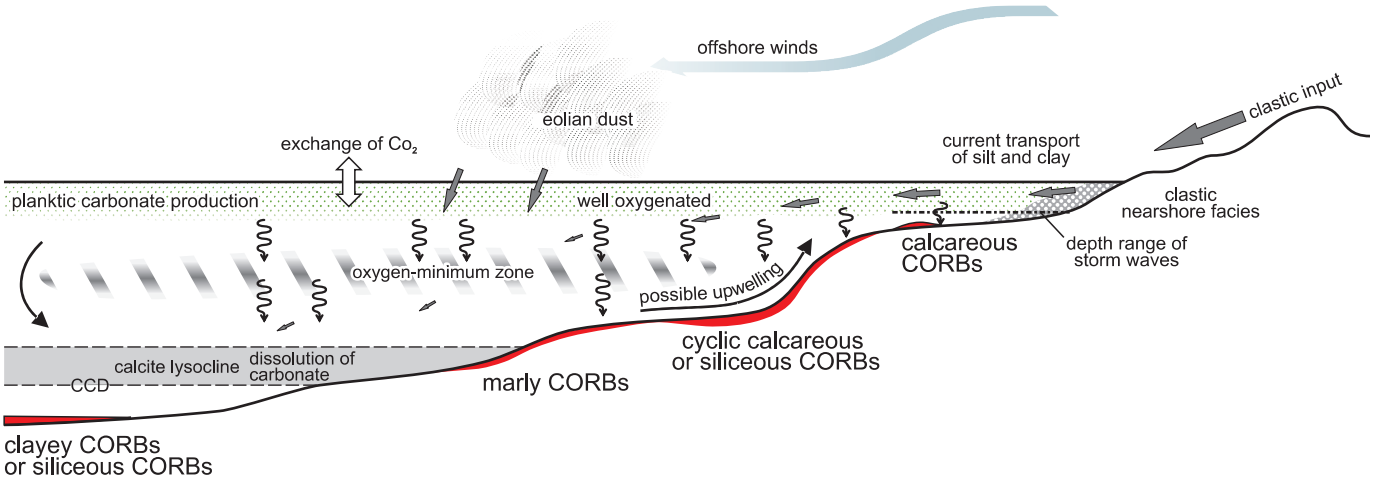

FIG. 5.—Overview of main depositional environments and main factors influencing CORB sedimentation in the pelagic–hemipelagic realm (based on Einsele and Ricken, 1991).

sions, such as in the Northern Calcareous Alps of Austria, indicate a preferential occurrence of CORBs only after considerable deepening into bathyal depths of several hundred meters of water depth, in accordance with observations by deep-sea drilling (Herbert et al., 1999). Sediment accumulation rates calculated both from biostratigraphic zones and from graphic correlation experiments for the different CORB settings range generally between 1 and 50 mm/kyr, with lower rates in pelagic clay settings comparable to recent deep-sea red clays, and higher values in hemipelagic carbonate or turbiditic settings, where clastic admixture is considerably greater.

CORB sedimentation was in opposition to clastic deep-water sedimentation. The general rule is that the greater the clastic input, the higher the sedimentation rate, and thus the decreased probability for CORB deposition. In detail, the relations are more complex: i.e., the fine-grained turbidites (Bouma Te divisions) or all or parts of submarine slides and large debris flows that can also be red colored and in places difficult to distinguish from autochthonous pelagic–hemipelagic CORBs (e.g., Krenmayr, 1996). The color of turbidites and hemipelagites in such a turbidite environment may depend on a complex interplay of various local and regional factors, such as the position of the oxidation–reduction level relative to the sea bottom, as well as ocean currents, oxidation by turbidite input, and sedimentation rates, and thus may vary over short horizontal distances within a given deep-water basin (Wagreich and Krenmayr, 2005). The presence of slump masses and pieces of red marlstones within overall gray successions proves a primary or at least a very early diagenetic origin of the red color.

Red claystone and shale intervals were deposited in orogenic flysch basins and at active continental margins only during times of low or missing clastic input (Skupien et al., this volume, Wagreich et al., this volume). In that respect, CORBs in such tectonically active basins characterize times of tectonic quiescence.

GEOCHEMISTRY

CORBs, like their gray-colored counterpart, are a complex mixture of terrigenous detritus, authigenic material, and biogenic material. Geochemical investigations on the distribution and abundance of the detrital and marine fractions of CORBs, as documented in this special publication and in previous publications, provide important information on the source region and ancient depositional environments.

According to data reported from Hu et al. (2005), the common geochemical property of CORBs is its extremely low organic-carbon content (usually less than 0.1%). However, the major chemical elements vary according to the lithology as indicated by the lithological classification (Fig. 4; Wagreich et al., this volume). Clayey CORBs are composed mostly of continent-derived clay minerals, the major elements of which are similar to those of modern oceanic red clays and to the World Shale Average (WSA; Wedepohl, 1971; Hu, 2002; Wang et al., 2005). Biogenous SiO_2 and $CaCO_3$ are the major nonterrigenous components of the siliceous and calcareous CORBs and other transitional CORBs of these three end members (Wagreich et al., this volume). Thus it is expected that the ratios between major terrigenous elements in all types of CORBs, such as K/Al or Ti/Al, are usually close to that of the World Shale Average (WSA, Wedepohl, 1971; Hu et al., this volume), though regional variations exist. More importantly, these values are usually quite stable in CORBs and adjacent rocks (Hu et al., this volume). This indicates that the source region usually did not change much during CORB deposition, and suggests that the red color is due to variation of chemical or physical factors in the depositional environment (Wang et al., 2005; Hu et al., 2005; Hu et al., 2006b, and references therein; Jansa and Hu, this volume).

The most important geochemical property of CORBs is the "iron anomaly" of fine-grained hematite (Eren and Kadir, 1999; Hu et al., 2006b; Hu et al., this volume). The direct geochemical proxy for this is the Fe^{3+}/Fe^{2+} ratio, which is always almost 50% higher in the red beds than in other colored rocks (Wang et al., 2005; Hu, 2002). The Fe/Al ratio of CORBs usually follows a close linear relationship, suggesting that the terrigenous source of iron has a higher Fe/Al ratio than that of non-red strata, including the World Shale Average (Huang et al., this volume). In addition, chemical sequential extractions of samples from Southern Tibet and the Austrian Alps (Neuhuber et al., 2007; Huang et al., this volume) indicate that ferric iron oxides (mainly hematite) are enriched and ferrous iron species, like pyrite and carbonate-associated iron are depleted in the red beds. This is contrary to the adjacent non-red sediments. The ratio between ferric oxides to total iron in the red beds is not only higher than in the adjacent non-red sediments but also is significantly higher than the aver-

age level of this ratio in Phanerozoic normal oxic sediments (Poulton and Raiswell, 2002). This indicates an oxygen-rich environment and slow deposition of red beds (Huang et al., this volume). Because of the coupling of the iron cycle and the phosphorus cycle, the excess burial of iron oxides in CORBs correspond to burial of more phosphorus and less recycled to seawater (Huang et al., 2007; Huang et al., this volume). Thus the paleo-productivity of the ocean decreases accordingly, because phosphorus is the ultimate limiting nutrient of marine production (Tyrrell, 1999).

Trace elements more accurately reflect conditions in the source area than do major elements. Trace elements also reflect paleoceanographic conditions. Case studies of the various CORB sections indicate that the ratios among the terrigenous trace elements and Al did not change significantly, which suggests little change in different source regions. Thus, paleoceanographic changes were the main reason for CORB deposition. However, in marine sediments such as CORBs, where organic carbon is poorly preserved, the relation between trace elements and paleoceanographic conditions is more complex. This is because many trace elements have both terrestrial and marine origins, and commonly the marine fraction was deposited together with organic matter (Piper and Isaacs, 1995). Generally the Al-normalization method is used to derive the marine fraction of the elements (Piper and Isaacs, 1995). Case studies in central Italy indicate that the Al-normalized levels of redox-sensitive elements such as U, V, Co, Cr, and Ni, are very low in the red sediments, suggesting an oxic depositional environment of CORBs (Hu et al., this volume). For example, Ni/Co-V/Cr and V/(V+Ni) - Fe^{3+}/Fe show that the red Scaglia Rosa Formation was deposited in a more oxic environment than the underlying white Scaglia Bianca Formation (Hu et al., this volume). In addition, nutrient-indicator trace elements, such as Cu, Zn, and Cd, are generally relatively depleted in the CORBs compared to the non-red sediments, which indicates more oligotrophic conditions. The paleo-productivity proxy, Ba, is lower in the red facies, signifying lower productivity. These properties suggest the oxygen-rich, oligotrophic nature of CORB deposition, and they have been documented in the Scaglia Rosa Formation of Italy (Hu et al., this volume) and the Chuangde Formation of Southern Tibet (Hu, 2002; Zou et al., 2005; Huang et al., this volume). Chemical sequential extraction results, along with the paleontological analyses of red beds in the Austrian Alps (Neuhuber et al., 2007; Ines Wendler et al., this volume), further validate these discoveries, where low productivity and highly oxic conditions of CORBs repeatedly succeeded the productive, less oxic conditions of the gray marl–limestone.

Rare earth elements (REE) in CORBs are reported only from Southern Tibet and Central Italy (Wang et al., 2005; Hu et al., this volume). A significant negative cerium anomaly (Ce^*) in the red beds indicates an oxic depositional environment. However, variation through the section does exist. In Southern Tibet, the Ce^* becomes negative at the base of the red beds, but the Ce^* gradually becomes less negative up section. On the other hand, in Central Italy the range is very similar to that of modern oxygenated oceanic seawater (0.1–0.;, Elderfield and Greaves, 1982). Hu et al. (this volume) interpret this as the inability of Ce to document the redox change: white and red limestones show almost the same negative Ce^* anomaly, ranging from 0.28 to 0.42. However, because the Ce* anomaly is also affected by the pH, i.e., the pCO_2 in the ocean, not only pO_2 (Liu et al., 1988), it is possible that the effect of the increase of pO_2 to Ce^* was offset by the decrease of pH as pCO_2, which may also increase due to more organic carbon oxidized in the ocean. Certainly this supposition deserves further study.

The relationship between carbon isotope excursions and the occurrences of CORBs is not as clear as for the oceanic anoxic events (OAEs), for which significant positive excursions characterize the carbon isotope record and indicate excess burial of organic carbon (Jenkyns et al., 1994; Tsikos et al., 2004). This might be partly due to the fact that CORBs are more diachronous and lasted longer than OAEs (Hu et al., 2005). The depositional environment may also contribute to this "ambiguity", because CORBs are mainly pelagic, deep-water facies, deposited in the slope to basin, which is not the primary place for burial of organic carbon (Katz et al., 2005). However, negative carbon isotope excursions were documented in the CORBs of several time slices: (1) CORBs of Upper Aptian, mid-Albian, mid-Cenomanian (ORB1, 4, and 8 of Hu et al., 2006a) and Upper Turonian age in the Umbria–Marche Basin, Central Italy (Stoll and Schrag, 2000); (2) Upper Turonian CORBs in the Eastern Alps of Austria (Neuhuber et al., 2007); (3) CORBs of uppermost Santonian–Campanian age in southern Tibet (Wang et al., 2005); and (4) Maastrichtian CORBs in the Romanian Carpathians (Bojar and Melinte, this volume). These negative excursions coincided either with the onset of CORB deposition, for example in Tibet and Austria, or with the color change from pink to red within the red beds (Bojar et al., this volume). Because the fluctuation of carbon isotopes in the marine carbonates was determined by the relative burial of fluxes of organic and inorganic carbon in the marine sediments (e.g., Kump and Arthur, 1999, and references therein), this suggests that productivity-driven changes in the flux of organic carbon to the bottom could have contributed to the red/gray/green/black color variation (Dean et al., 1984; Wortmann et al., 1999).

Other geochemical studies on CORBs include oxygen-isotope and organic geochemistry. However, direct measurements of oxygen isotopes in CORBs is rare because oxygen isotopes are prone to diagenesis (Stoll and Schrag, 2000). Data from the Austrian Alps, for example, show that positive excursions accompanied the onset of CORB deposition (Neuhuber et al., 2007), which may be related to the Late Cretaceous cooling trend (MacLeod and Huber, 1996). The single organic-geochemistry study is from Southern Tibet (Zou et al., 2005), which reported lower *n17/n27* and *nC17*/hopane ratios for the red beds, which suggests that a mixture of bacterial and terrestrial remains is preserved in these beds. The extremely low content of organic carbon in the red beds makes organic-geochemical study difficult, e.g., the TOC contents of the CORBs from the Chuangde Formation are mostly less than 0.1% (Zou et al., 2005).

In summary, CORBs are a mixture of terrestrial, seawater-derived, and biogenous material according to the most updated geochemical data. The most significant geochemical features of CORBs are enrichment of ferric oxides and depletion of organic carbon and redox-sensitive trace elements, while other continent-derived major and trace elements vary much less. Several negative carbon isotope excursions have also been documented in the red beds. These geochemical features together with other data presented in the above sections characterize the paleoclimatic and paleoceanographic significance of red beds.

PALEOCLIMATIC AND PALEOCEANOGRAPHIC IMPLICATIONS

Three types of deep-water red sediments have been proposed up to now: (1) oxidized detrital debris introduced by mass flow (e.g., Lajoie and Chagnon, 1973), (2) modern oceanic red clays deposited below the CCD (Glasby, 1991), and (3) iron-bacteria-mediated red limestone under suboxic conditions (Mamet and Préat, 2006, and references therein). However, CORBs cannot easily be classified into these three categories because most are

not mass-gravity deposits, nor were they formed under suboxic conditions like iron-bacteria-mediated red limestone (Hu et al., 2005, 2006a). Although some CORBs, for example the Plantagenet Formation in the central North Atlantic, are similar to modern oceanic red clays (Jansa and Hu, this volume), deposition of these clays is limited to the central parts of large oceanic basins where productivity and sedimentation rates were extremely low (Glasby, 1991). This genesis does not account for features of most calcareous CORBs such as those in the Austrian Alps (Wagreich et al., this volume). Thus the genesis of CORBs must be redefined in order to elucidate their paleoclimatic and paleoceanographic significance.

In order to resolve this problem, paleoceanographic conditions of CORB deposition must be known. According to the previous sections of this chapter, no matter what the lithology and depositional environments, CORBs are characterized by enrichment of ferric oxides, depletion of redox-sensitive and nutrient-like trace elements, locally negative excursions of carbon isotopes, and almost no change in terrigenous fractions. These factors indicate that CORBs were deposited under highly oxic, oligotrophic, and probably low-productivity conditions. The micropaleontological data also support this conclusion (Kuhnt and Moullade, 1991; Kuhnt and Holbourne, 2005; Bojar and Melinte, this volume; Ines Wendler et al., this volume). This conclusion is further corroborated by comparing integrated data of dissolved-oxygen index (Kaiho, 1994), phosphorus burial (Föllmi, 1996), carbon isotopes (Erba, 2004), ocean crust production (IPSC Scientific Planning Working Group, 2001), and organic-carbon burial based on geochemical modeling (Hanson and Wallmann, 2003) (Fig. 6). The dissolved-oxygen index (DOI) was characterized by a large and abrupt fall at the Cenomanian–Turonian boundary related to the OAE2 and then generally high levels from the Turonian to the early Maastrichtian, which indicate an oxic deep ocean during the Late Cretaceous (Kaiho, 1994). Records of phosphorus burial and carbon isotopes generally show excursions at OAEs, suggesting eutrophication and enhanced productivity, and numerous "valleys" (possible oligotrophic) between these excursions. According to the comprehensive geochemical modeling of organic-carbon burial (Hanson and Wallmann, 2003), the level of organic-carbon burial was high from OAE1a to OAE2 (forming the plateau) but decreased rapidly from OAE2 onwards, with a local minimum in the Santonian–Campanian. This modeling result is consistent with the significant global increase in inorganic/organic-carbon burial ratio of $68 \times 10^{18} / 16 \times 10^{18}$ kg · yr^{-1} (4.25:1) in the Early Cretaceous to $133 \times 10^{18} / 20 \times 10^{18}$ kg · yr^{-1} (6.65/1) in the Late Cretaceous according to the abundance of organic carbon in the marine sediments (Budyko et al., 1987). All of these data indicate that CORB deposition was under highly oxic and oligotrophic conditions with possibly lower productivity and much less organic-carbon burial.

The highly oxic conditions and wide geographic distribution of CORBs may suggest active ocean circulation. Great efforts have been made to decipher ocean circulation, with fruitful results by numerical modeling (Hay, this volume, and references therein). Ocean models suggest three regions that might have been sites of deep convection, i.e., open-ocean deep-water formation during the Cretaceous: (1) the Arctic, (2) the northeastern Tethys, and (3) the Antarctic margin between South America and Australia (Brady et al., 1998; Otto-Bliesner et al., 2002). In these models paleogeography may have had an important effect on the ocean circulation. According to paleogeographic reconstructions (Hay et al., 1999), no deep connections were present among the Pacific, the western Tethys, and the Arctic in the Early Cretaceous. The North and South Atlantic became connected and exchanged surface and shallow waters in the Albian–Cenomanian (112–94 Ma) and the deep-water connection was delayed until 90 to 70 Ma (Poulsen et al., 2003). Another notable feature of the Late Cretaceous ocean is the possible existence of a Tethyan clockwise gyre (Bush, 1997; Poulsen et al., 1998; Hotinski and Toggweiler, 2003), which may also have contributed to ventilation of the deep ocean, especially in the western Tethys (Bush, personal communication, 2004). The Nd isotope data attest to an increased Pacific influence in the surface waters of the eastward current during the Albian onward when the successive opening of the North and South Atlantic ultimately strengthened this current (Puceat et al., 2005). As a whole these modeling and geochemical data indicate that ocean circulation was very active during the Late Cretaceous at the time when CORBs were globally distributed.

However, these models are usually limited to a specific time slice, and thus cannot account for the "continuous" features of ocean circulation. In this aspect the paleo-temperature records can give some indication because ocean circulation is closely related to temperature. Numerous studies indicate that mid- to Late Cretaceous climate was characterized by an equable warm greenhouse that was interrupted by brief fluctuations, for example the thermal maximum around the Cenomanian–Turonian boundary (Cretaceous thermal maximum; Poulsen et al., 2003) and a series of cooling pulses in Late Aptian (including the Aptian–Albian boundary), mid-Cenomanian, Late Turonian, Early Campanian, Campanian–Maastrichtian boundary, mid-Maastrichtian, and end-Maastrichtian (Frakes, 1999; Huber et al., 2002; Royer, 2006). Secular trends also existed, such as the long-term temperature decrease since the Cenomanian–Turonian boundary, lasting until the end of Cretaceous (Stoll and Schrag, 2000; Clarke and Jenkyns, 1999), which may have been due to reduction of CO_2 because of decreased ocean-floor volcanism and huge burial of organic carbon during OAEs (Larson, 1991; Arthur et al., 1988). The occurrences of CORBs are related to the paleoclimatic history of the mid-Cretaceous; Aptian–Cenomanian CORBs correspond approximately to brief cool interludes. The onset of Turonian CORB deposition in many basins after OAE2 coincides with the cooling interludes in the early Late Turonian (e.g., Bornemann et al., 2008). These comparisons show that climate cooling might have been part of the reason for the occurrences, duration, and wide distribution of CORBs during this period, because ocean circulation is more active and thus better ventilated with a higher equator-to-pole temperature gradient (Hay et al., 1999).

Effective ventilation of the ocean would have an important effect on the behavior of nutrients like phosphorus. Positive feedback between anoxia and increased productivity of the ocean has been suggested to explain the occurrences of OAEs (van Cappellen and Ingall, 1994; Nederbragt et al., 2004): when the deep oceans become anoxic, more phosphorus is returned to the seawater, which leads to higher productivity; then higher productivity results in further anoxia, and so on. Even in the oxic ocean, burial efficiency of phosphorus is related to the redox conditions in the sediments, i.e., the more oxic, the higher the burial efficiency of phosphorus (Colman and Holland, 2000), which leads to a less productive ocean and therefore more oxic conditions in the deep ocean. Thus the redox-sensitive behavior of phosphorus helps explain the oligotrophic condition of CORB deposition and lower productivity during the Late Cretaceous (Huang et al., 2007).

From the preceding discussion it is clear that CORBs were closely related to the evolution of the Cretaceous Earth system. The deposition and wide distribution of CORBs were related to paleoclimate, paleogeography, ocean currents, nutrient cycles, and low sediment accumulation rates (Jansa and Hu, this vol-

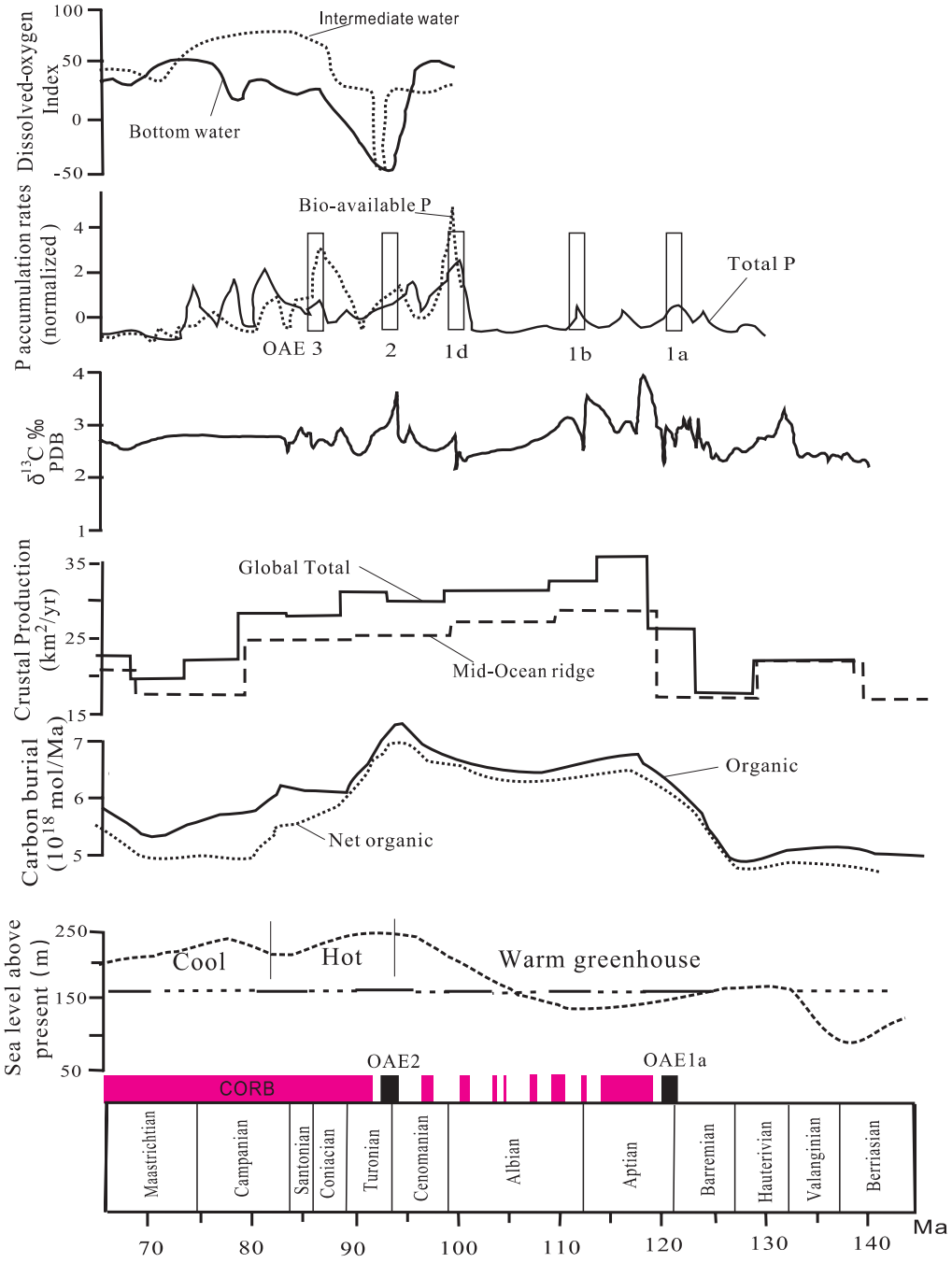

FIG. 6.—Integrated records indicating Cretaceous global climatic–oceanic change. Carbon isotope data are from Erba (2004) and references therein; dissolved-oxygen index, P accumulation rates, and organic-carbon burial rates are from Kaiho (1994), Föllmi (1996), and Hanson and Wallmann (2003), respectively. Crustal production rates, sea-level change, and duration of black shales are cited from IPSC Scientific Planning Working Group (2001). Blue arrows indicate cooling periods, and red arrows show the warmer phase (data from Lees, 2002).

ume), among other processes during the Late Cretaceous. These factors can be organized into a more precise model that explains how they contributed to the wide time–space distribution of CORBs. The development of the paleogeographic configuration provides the basis for the ventilation of the deep ocean, which was strengthened by the climate cooling. The behavior of redox-sensitive nutrient elements like phosphorus further stimulated the development of oligotrophic conditions. All of these factors contributed to the wide, even global distribution of CORBs.

CONCLUSIONS

Although the first report of Cretaceous marine red beds was more than one hundred years ago (Štur, 1860), limited research

efforts into that topic followed, so the study of CORBs is still in its infancy. The most valuable contribution of the two IGCP projects, however, is not in their academic achievements proven by the recent published papers, articles, and conference abstracts. More importantly, the two IGCP projects have provided a solid framework for future research. These projects have shown the significance of oceanic red beds and have generated interest among scientists of the world in the study of CORBs. The genesis and paleoceanographic and paleoclimatological significance of CORBs are relevant to expanding the present knowledge of Earth system science. Multidisciplinary investigations and further correlation of CORB data are still needed in the near future. The initiation of IGCP project 555, "Rapid environmental/climate change in the Cretaceous greenhouse world: land–ocean interactions" may serve to achieve part of this goal. Therefore the present publication on the genesis of CORBs should not be the last.

Bearing this in mind, the following points can be made to summarize our present understanding of CORBs:

1. CORBs are red to pink to brown, fine-grained sedimentary rocks of Cretaceous age deposited in pelagic marine environments. Their lithology includes red shales, red marls, finedgrained limestones, or red cherts, and can be described and classified in the context of deep-water pelagic and hemipelagic sedimentary systems. This definition of oceanic red beds excludes red sediments that were derived from erosion of continental red beds and transported from continental to marine environments.

2. CORBs are globally distributed in outcrops in Europe, Asia, Africa, New Zealand, the Caribbean, and at DSDP and ODP sites in the Tethyan Atlantic, Pacific, and Indian oceans. CORBs experienced two paleogeographical expansions in the middle Aptian CC7 zone just shortly after the OAE1a and CC11 after the latest Cenomanian OAE2, respectively. Lower Cretaceous CORB outcrops are very much less common. CORBs were limited regionally in Aptian to Cenomanian strata, occurring as discrete thin beds. After the OAE2, CORBs cropped out in 25 basins or tectonic zones beginning in the CC11 zone; during zones CC13–CC15 (Coniacian–Early Santonian) CORB deposition was at its maximum in up to 34 basins or tectonic zones in the world. Similar CORB distribution happens in the DSDP and ODP oceanic sites.

3. Diverse paleontological data, including planktic foraminifera, nannofossils, agglutinated foraminifera, dinoflagellates, and radiolaria, were investigated from the CORB sections to document the biostratigraphic position and to constrain the ages of CORBs. Two approaches were taken to interpolate numerical ages on the bases and tops of marine red beds. The bases and tops of biozones were interpolated into the recently revised Cretaceous time scales. A second method to interpolate ages was by graphic correlation of selected CORB sections with the MIDK42 chronostratigraphic database. The two methods result in comparable age ranges, although graphic correlation generates more precise ages.

4. Mineralogical studies on the CORBs show that the red color of the CORBs, whether their lithology is shale, marl, or limestone, is due to the presence of microscopic, very finely dispersed hematite. The hematite could be very early diagenetic in origin, related to highly oxic conditions.

5. Case studies of CORBs indicate three general facies types: deep-water red claystones deposited below the calcite compensation depth, red hemipelagic and pelagic carbonates, and red cherts and radiolarites. A ternary classification is suggested with the end members clay, carbonate, and chert. The depositional environments of most CORBs were in relatively deep oceanic basins and pelagic in the sense that these environments were generally far from shorelines and were not associated with coarse terrigenous clastic facies. Low sediment accumulation rates and great paleo–water depth were significant controlling factors of CORBs, although the relationship is more complex in specific basins, as described in this compilation.

6. The common geochemical properties of CORBs are their extremely low organic-carbon content and high level of ferric oxides. The ratio of ferric oxides to total iron is not only higher than the level of adjacent non-red sediments, but it is also higher than that of Phanerozoic normal marine oxic sediments. The iron ratio, together with other major-element, trace-element, and isotope data, suggest highly oxic sediment conditions and oligotrophic, low-productivity water masses possibly associated with cooler climates.

7. Deposition and the wide geographic distribution of CORBs were related to climate, paleogeography, ocean currents, and nutrient cycles, among other factors, in the Late Cretaceous. The development of the paleogeographic setting provided the paleobathymetry for ventilation of the deep ocean and made deposition of CORBs possible. Then the climatic cooling could have strengthened the ocean circulation, pumping more oxic waters to the sediment–water interface. The fixation of redox-sensitive nutrient elements like phosphorus further stimulated the development of oligotrophic conditions, causing low productivity in the ocean. All of these factors contributed to the wide, even global distribution of CORBs.

ACKNOWLEDGMENTS

This paper was possible only with the generous support of data and open discussion of our IGCP colleagues, including Krzysztof Bak, Marta Bak, Rufus Bertle, Miroslav Bubik, Hans Egger, Karl Föllmi, Willam W. Hay, Dan Hikuroa, Luba Jansa, Wolfgang Kuhnt, Xianghui Li, Ewa Malata, Mihaela C. Melinte, Haydon P. Mort, Stephanie Neuhuber, Massimo Sarti, Petr Skupien, Lilian Švábenická, Okan Tüysüz, Xiaoqiao Wan, Ines Wendler, Jens Wendler, and Ismail Yilmaz, among others. Special thanks are to given our many colleagues for their frank discussion at the IGCP meetings. Mr. Chen Xi and Mr. Wang Pingkang are thanked for their help in dealing with DSDP and ODP site information and preparing Figure 1. This work is supported by the Chinese MOST 973 (2006CB701400) and the NSFC project (40332020), and is a contribution to IGCP 463 and IGCP 494, the two projects of International Geosciences Program of UNESCO & IUGS.

REFERENCES

ALSEN, P., AND SURLYK, F., 2004, Deep marine red beds of the Valanginian–Hauterivian (Lower Cretaceous) of East Greenland: Palaeo-oceanographic implications (abstract): 32nd International Geological Congress, Session T29.10, Abstracts.

ARTHUR, M.A., 1979, Origin of Upper Cretaceous multicolored claystones of the western Atlantic, *in* Tucholke, B.E., Vogt, P.R., et al., eds., Initial Reports of the Deep Sea Drilling Project, v. 43: Washington, D.C., U.S. Government Printing Office, p. 417–420.

ARTHUR, M.A., AND FISCHER, A.G., 1977, Upper Cretaceous–Paleocene magnetic stratigraphy at Gubbio, Italy I. Lithostratigraphy and sedimentology: Geological Society of America, Bulletin, v. 88, p. 367–371.

ARTHUR, M.A., DEAN, W.E., AND PRATT, L.M., 1988, Geochemical and climatic effects of increased marine organic carbon burial at the Cenomanian/Turonian boundary: Nature, v. 335, p. 714–717.

BAK, K., 2002, Cretaceous oceanic red beds in southern Poland, *in* Hu, X., and Sarti, M., eds., Cretaceous Oceanic Red Beds (CORBs) in an Apennines–Alps–Carpathians Transect: Field Guidebook for Inaugural Workshop of IGCP 463, Ancona, Italy, p. 73–115.

BORNEMANN, A., NORRIS, R.D., FRIEDRICH, O., BECKMANN, B., SCHOUTEN, S., SINNINGHE DAMSTÉ, J.S., VOGEL, J., HOFMANN, T., AND WAGNER, T., 2008, Isotopic evidence for glaciation during the Cretaceous Supergreenhouse: Science, v. 319, p. 189–192.

BRADY, E.C., DECONTO, R.M., AND THOMPSON, S.L., 1998, Deep water formation and poleward ocean heat transport in the warm climate extreme of the Cretaceous (80 Ma): Geophysical Research Letters, v. 25, p. 4205–4208.

BUDYKO, M.I., RONOV, A.B., AND YANSHIN, A.L., 1987, History of the Earth's Atmosphere: Berlin, Springer-Verlag, 139 p.

BURNETT, J.A., 1998, Upper Cretaceous, *in* Bown, P.R., ed., Calcareous Nannofossil Biostratigraphy: London, Chapman & Hall, p. 132–199.

BUSH, A.B.G., 1997, Numerical simulation of the Cretaceous Tethys circumglobal current: Science, v. 275, p. 807–810.

CHANNELL, J.E.T., FREEMAN, R., HELLER, F., AND LOWRIE, W., 1982, Timing of diagenetic haematite growth in red pelagic limestones from Gubbio (Italy): Earth and Planetary Science Letters, v. 58 p. 189–201.

CHEN, X., WANG, C.S., HU, X.M., ET AL., 2007, Global correlation of Cretaceous oceanic red beds: Acta Geologica Sinica (English Edition), v. 81(6), p. 1070–1086.

CLARKE, L.J., AND JENKYNS, H.C., 1999, New oxygen isotope evidence for long-term Cretaceous climatic change in the Southern Hemisphere: Geology, v. 27, p. 699–702.

COLMAN, A.S., AND HOLLAND, H.D., 2000, The global diagenetic flux of phosphorus from marine sediments to the oceans: redox sensitivity and the control of atmospheric oxygen levels, *in* Glenn, C.R., Prévôt-Lucas, L., and Lucas, J., eds., Marine Authigenesis: From Global to Microbial: SEPM, Special Publication 66, p. 53–75.

DEAN, W.E., ARTHUR, M.A., AND STOW, D.A.V., 1984, Origin and geochemistry of Cretaceous deep-sea black shales and multicolored claystones, with emphasis on deep sea drilling project site 530, southern Angola basin, *in* Hay, W.W., Sibuet, J.-C., et al., eds., Initial Reports of the Deep Sea Drilling Project, v. 75: Washington, D.C., U.S. Government Printing Office, p. 819–830.

DULIC, I., AND BOGICEVIC, G., 2002, Upper Cretaceous red beds of Vojvodna (Northern Serbia): Inaugural Workshop of IGCP 463, Ancona, Italy, Programme and Abstracts, p. 4.

EINSELE, G., AND RICKEN, W., 1991, Limestone–marl alternations—an overview, *in* Einsele, G., Ricken, W., and Seilacher, A., eds., Cycles and Events in Stratigraphy: Berlin, Springer, p. 23–47.

ELDERFIELD, H., AND GREAVES, M.J., 1982, The rare earth elements in seawater: Nature, v. 296, p. 214–219.

ERBA, E., 2004, Calcareous nannofossils and Mesozoic oceanic events: Marine Micropaleontology, v. 52, p. 85–106.

ERBA, E., CHANNELL J.E.T., CLAPS, M., JONES, C., LARSON, R.L., OPDYKE, B., PREMOLI SILVA, I., RIVA, A., SALVINI, G., AND TORRICELLI, S., 1999, Integrated stratigraphy of the Cismon Apti-core (Southern Alps, Italy): a 'reference section' for the Barremian–Aptian interval at low latitudes: Journal of Foraminiferal Research, v. 29, p. 371–391.

EREN, M., AND KADIR, S., 1999, Colour origin of Upper Cretaceous pelagic red sediments within the Eastern Pontides, northeast Turkey: International Journal of Earth Sciences, v. 88, p. 593–595.

FÖLLMI, K.B., 1996, The phosphorus cycle, phosphogenesis and marine phosphate-rich deposits: Earth-Science Reviews, v. 40, p. 55–124.

FRAKES, L.A., 1999, Estimating the global thermal state from Cretaceous sea surface and continental temperature data, *in* Barrera, E., and Johnson, C.C., eds., Geological Evolution of the Cretaceous Ocean–Climate System: Geological Society of America, Special Paper 332, p. 49–57.

GLASBY, G.P., 1991, Mineralogy, geochemistry, and origin of Pacific red clays: a review: New Zealand Journal of Geology and Geophysics, v. 34, p. 167–176.

HABIB, D., AND DRUGG, W.S., 1987, Palynology of sites 603 and 605, Leg 93, Deep Sea Drilling Project, *in* van Hinte, J.E., Wise, S.W., Jr., et al., eds., Initial Reports of the Deep Sea Drilling Project, v. 93: Washington, D.C., U.S. Government Printing Office, p. 751–766.

HANSON, K.W., AND WALLMANN, K., 2003, Cretaceous and Cenozoic evolution of seawater composition, atmospheric O_2 and CO_2: a model perspective: American Journal of Science, v. 303, p. 94–148.

HARDENBOL, J., AND ROBASZYNSKI, F., 1998, Introduction to the Upper Cretaceous, *in* de Graciansky, P.-C., Hardenbol, J., Jacquin, T., and Vail, P.R., eds., Mesozoic and Cenozoic Sequence Stratigraphy of European Basins: SEPM, Special Publication 54, p. 329–332.

HARLAND, W.B., COX, A.V., AND LLEWELLYN, P.G., 1990, A Geologic Time Scale 1989: Cambridge, U.K., Cambridge University Press, 263 p.

HAY, W.W., DECONTO, R.M., WOLD, C.N., WILSON, K.M., VOIGT, S., SCHULZ, M., WOLD, A.R., DULLO, W-CHR., RONOV, A.B., BALUKHOVSKY, A.N., AND SÖDING, E., 1999, An alternative global Cretaceous paleogeography, *in* Barrera, E., and Johnson, C.C., eds., Evolution of the Cretaceous Ocean–Climate System: Geological Society of America, Special Paper 332, p. 1–47.

HERBERT, T.D., GEE, J., AND DIDONNA, S., 1999, Precessional cycles in Upper Cretaceous pelagic sediments of the South Atlantic: Long-term patterns from high-frequency climate variations, *in* Barrera, E., and Johnson, C.C., eds., Evolution of the Cretaceous Ocean–Climate System: Geological Society of America, Special Paper 332, p. 105–120.

HOTINSKI, R.M., AND TOGGWEILER, J.R., 2003, Impact of a Tethyan circumglobal passage on ocean heat transport and ''equable'' climates: Paleoceanography, v. 18, p. 1007, doi:10.1029/2001PA000730.

HU, X.M., 2002, Sedimentary geology of Cretaceous in southern Tibet, and the Upper Cretaceous oceanic red beds: unpublished Ph.D. thesis, Chengdu University of Technology, China, 216 p.

HU, X.M., JANSA, L., WANG, C.S., SARTI, M., BAK, K., WAGREICH, M., MICHALIK, J., AND SOTÁK, J., 2005, Upper Cretaceous oceanic red beds (CORBs) in the Tethys: occurrences, lithofacies, age, and environments: Cretaceous Research, v. 26, p. 3–20.

HU, X.M., JANSA, L., AND SARTI, M., 2006a, Mid-Cretaceous oceanic red beds in the Umbria–Marche Basin, central Italy: Constraints on paleoceanography and paleoclimate: Palaeogeography, Palaeoclimatology, Palaeoecology, v. 233, p. 163–186.

HU, X.M., WANG, C.S., LI, X.H., AND JANSA, L., 2006b, Upper Cretaceous oceanic red beds in southern Tibet: Lithofacies, environments and colour origin: Science in China, Series D, Earth Sciences, v. 49, p. 785–795.

HUANG Y.J., WANG C.S., ADATTE, T., AND WANG, Y.L., 2007, Phosphorus speciation in Cretaceous strata from south Tibet: Acta Geologica Sinica (English Edition), v. 81(6), p. 1012–1018.

HUBER, B.T., NORRIS, R.D., AND MACLEOD, K.G., 2002, Deep-sea paleo-temperature record of extreme warmth during the Cretaceous: Geology, v. 30, p. 123–126.

IPSC SCIENTIFIC PLANNING WORKING GROUP, 2001, Earth, Oceans and Life—Integrated Ocean Drilling Program Initial Science Plan, 2003–2013, 110 p.

JENKYNS, H.C., GALE A.S., AND CORFIELD, R.M., 1994, Carbon and oxygen isotope stratigraphy of the English Chalk and Italian Scaglia and its paleoclimatic significance: Geological Magazine, v. 131, p. 1–34.

JOHNSSON, M.J., AND REYNOLDS, R.C., 1986, Clay mineralogy of shale–limestone rhythmites in the Scaglia Rossa (Turonian–Eocene), Italian Apennines: Journal of Sedimentary Petrology, v. 56, p. 501–509.

KAIHO, K., 1994, Planktonic and benthic foraminiferal extinction events during the last 100 m.y.: Palaeogeography, Palaeoclimatology, Palaeoecology, v. 111, p. 45–71.

KATZ, M.E., WRIGHT, J. D., MILLER, K.G., CRAMER, B.S., FENNEL, K., AND FALKOWSKI, P.G., 2005, Biological overprint of the geological carbon cycle: Marine Geology, v. 217, p. 323–338.

KRENMAYR, H.G., 1996, Hemipelagic and turbiditic mudstone facies associations in the Upper Cretaceous Gosau Group of the Northern Calcareous Alps (Austria): Sedimentary Geology, v. 101, p. 149–172.

KUHNT, K., AND HOLBOURN, A., 2005, Late Cretaceous deep-water benthic foraminiferal biofacies and lithofacies of western and eastern Tethys: Earth Science Frontier, v. 26, p. 81–104 (in Chinese with English abstract).

KUHNT, W., AND MOULLADE, M., 1991, Quantitative analysis of Upper Cretaceous abyssal agglutinated foraminiferal distribution in the North Atlantic–paleoceanographic implications: Revue de Micropaléontologie, v. 34, p. 313–349.

KUHNT, W., MOULLADE, M., AND KAMINSKI, M.A., 1996, Cretaceous palaeoceanographic events and abyssal agglutinated foraminifera, *in* Moguilevsky, A., and Whatley, R., eds., Microfossils and Oceanic Environments: University of Wales, Aberystwyth Press, p. 63–75.

KUMP, L.R., AND ARTHUR, M.A., 1999, Interpreting carbon-isotope excursions, carbonates and organic matter: Chemical Geology, v. 161, p. 181–198.

LAJOIE, J., AND CHAGNON, A., 1973, Origin of red beds in a Cambrian flysch sequence, Canadian Appalachians, Quebec: Sedimentology, v. 20, p. 91–103.

LARSON, R.L., 1991, Latest pulse of Earth: Evidence for a mid-Cretaceous super plume: Geology, v. 19, p. 547–550.

LEES, A.J., 2002, Nannofloral biogeographic patterns illustrate long-term climate change: warming/cooling trends in the Late Cretaceous Indian and Pacific Oceans, *in* Bice, K.L., Bralower, T.J., Duncan, R.A., Huber, B.T., Leckie, R.M., and Sageman, B.B., eds., Cretaceous Climate–Ocean Dynamics: Future Directions for IODP, a JOI/USSSP and NSF Sponsored Workshop, The Nature Place, Florissant, Colorado, U.S.A. (abstract), p. 52.

LIU, Y.G., SCHMITT, R.A., AND MIAH, M.R.U., 1988, Cerium: a chemical tracer for paleo-oceanic redox conditions: Geochimica et Cosmochimica Acta, v. 52, p. 1361–1371.

MACLEOD, K.G., AND HOPPE, K.A., 1992, Evidence that inoceramid bivalves were benthic and harbored chemosynthetic symbionts: Geology, v. 20, p. 117–120.

MACLEOD, K.G., AND HUBER, B.T., 1996, Testing for an oceanic role in creating low latitudinal temperature gradients during Cretaceous warmth: North American Paleontological Convention (NAPC-96), Paleontological Society, Special Publication 8, p. 253.

MACLEOD, K.G., HUBER, B.T., AND WARD, P.D., 1996, The biostratigraphy and paleobiogeography of Maastrichtian inoceramids, *in* Ryder, G., Fastovsky, D., and Gartner, S., eds., The Cretaceous–Tertiary Event and Other Catastrophes in Earth History: Geological Society of America, Special Paper 307, p. 361–373.

MACLEOD, K.G., HUBER, B.T., PLETSCH, T., RÖHL, U., AND KUCERA, M., 2001, Maastrichtian foraminiferal and paleoceanographic changes on Milankovitch timescales: Paleoceanography, v. 16, p. 133–154.

MAMET, B., AND PRÉAT, A., 2006, Iron-bacterial mediation in Phanerozoic red limestones: State of the art: Sedimentary Geology, v. 185, p. 147–157.

MELINTE, M.C., AND JIPA, D.C., 2005, Campanian–Maastrichtian marine red beds in Romania: biostratigraphic and genetic significance: Cretaceous Research, v. 26, p. 49–56.

MITCHELL, S.F., 1995, Lithostratiography and biostratigraphy of the Hunstanton Formation (Red Chalk, Cretaceous) succession at Speeton, North Yorkshire: Yorkshire Geological Society, Proceedings, v. 52, p. 107–112.

NEDERBRAGT, A.J., THUROW, J., VONHOF, H., AND BRUMSACK, H.J., 2004, Modelling oceanic carbon and phosphorus fluxes: implications for the cause of the late Cenomanian Oceanic Anoxic Event (OAE2): Geological Society of London, Journal, v. 161, p. 721–728.

NEUHUBER, S., WAGREICH, M., WENDLER, I., AND SPÖTL, C., 2007, Turonian Oceanic Red Beds in the Eastern Alps: Concepts for palaeoceanographic changes in the Mediterranean Tethys: Palaeogeography, Palaeoclimatology, Palaeoecology, v. 251, p. 222–238.

OGG, J.G., AGTERBERG, F.P., AND GRADSTEIN, F.M., 2004, The Cretaceous Period, *in* Gradstein, F.M., Ogg, J.G., and Smith, A.G., eds., A Geologic Time Scale 2004: Cambridge, U.K., Cambridge University Press, p. 344–383.

OTTO-BLIESNER, B.L., BRADY, E.C., AND SHIELDS, C., 2002, Late Cretaceous ocean: Coupled simulations with National Center for Atmospheric Research Climate System Model: Journal of Geophysical Research, v. 107, no. D2, 10.1029/2001DJ000821.

PERCH-NIELSEN, K., 1985, Cenozoic calcareous nannofossils, *in* Bolli, H.M., Saunders, J.B., and Perch- Nielsen, K., eds., Plankton Stratigraphy: Cambridge, U.K., Cambridge University Press, p. 427-554.

PIPER, D.Z., AND ISAACS, C.M., 1995, Geochemistry of minor elements in the Monterey Formation, California—seawater chemistry of deposition: U.S. Geological Survey, Professional Paper 1566, 41 p.

POULSEN, C.J., GENDASZEK, A.S., AND JACOB, R.L., 2003, Did the rifting of the Atlantic Ocean cause the Cretaceous thermal maximum?: Geology, v. 31, p. 115–118.

POULSEN, C.J., SEIDOV, D., BARRON, E.J., AND PETERSON, W.H., 1998, The impact of paleogeographic evolution on the surface oceanic circulation and the marine environment within the mid-Cretaceous Tethys: Paleoceanography, v. 13, p. 546–559.

POULTON, W.S., AND RAISWELL, R., 2002, The low-temperature geochemical cycle of iron: from continental fluxes to marine sediment deposition: American Journal of Science, v. 302, p. 774–805.

PUCEAT, E., LECUYER, C., AND REISBERG, L., 2005, Neodymium isotope evolution of NW Tethyan upper ocean waters throughout the Cretaceous: Earth and Planetary Science Letters, v. 236, p. 705–720.

ROYER, D.L., 2006, CO_2-forced climate thresholds during the Phanerozoic: Geochimica et Cosmochimica Acta, v. 70, p. 5665–5675.

SISSINGH, W., 1977, Biostratigraphy of Cretaceous calcareous nannoplankton: Geologie en Minbouw, v. 56, p. 37–65.

STOLL, H.M., AND SCHRAG, D.P., 2000, High-resolution stable isotope records from the Upper Cretaceous rocks of Italy and Spain: Glacial episodes in a greenhouse planet?: Geological Society of America, Bulletin, v. 112, p. 308–319.

STOW, D.A.V., READING, H.G., AND COLLINSON, J.D., 1996, Deep seas, *in* Reading, H.G., ed., Sedimentary Environments; Processes, Facies and Stratigraphy, Third Edition: Oxford, U.K., Blackwell, p. 395–453.

ŠTUR, D., 1860, Bericht über die geologische Übersichts—Aufnahme d. Wassergebietes der Waag und Meutra: Geologische Reichsanstalt, Jahrbuch, v. 11, p. 17–149.

THUROW, J., MOULLADE, M., BRUMSACK, H.J., MAURE, E., TAUGOURDEAU-LANTZ, J., AND DUNHAM, K., 1988, The Cenomanian/Turonian boundary event (CTBE) at Hole 641A, ODP Leg 1 03 (Compared with the CTBE interval at Site 398), *in* Boillot, G., Winterer, E.L., et al., eds., Proceedings of the Ocean Drilling Program, Scientific Results: College Station, TX, v. 103, p. 58–617.

TSIKOS, H., JENKYNS, H.C., AND WALSWORTH-BELL, B., 2004, Cenomanian–Turonian carbon-isotope stratigraphy recorded by the Cenomanian–Turonian oceanic anoxic event: Correlation and implications based on three key locations: Geological Society of London, Journal, v. 161, p. 711–719.

TYRRELL, T., 1999, The relative influences of nitrogen and phosphorus on oceanic primary production: Nature, v. 400, p. 525–531.

VAN CAPPELLEN, P., AND INGALL, E.D., 1994, Benthic phosphorus regeneration, net primary production and ocean anoxia: A model of coupled marine biogeochemical cycles of carbon and phosphorus: Paleoceanography, v. 9, p. 677–692.

VAN HOUTEN, F.B., 1964, Origin of red beds—some unresolved problems, *in* Nairn, A.E.M., ed., Problems in Paleoclimatology: New York, Interscience, p. 647–661.

WAGREICH, M., AND KRENMAYR, H.G., 2005, Upper Cretaceous oceanic red beds (CORBs) in the Northern Calcareous Alps (Nierental Formation, Austria): slope topography and clastic input as primary controlling factors: Cretaceous Research, v. 26, p. 57–64.

WAGREICH, M., PAVLISHINA, P., AND MALATA, E., 2006, Biostratigraphy of the lower red shale interval in the Rhenodanubian flysch zone of Austria: Cretaceous Research, v. 27, p. 743–753.

WAN, X., LAMOLDA, M.A., SI, J., AND LI, G., 2005, Foraminiferal Stratigraphy of Late Cretaceous red beds in southern Tibet: Cretaceous Research, v. 26, p. 43–48.

WANG, C.S., HU, X.M., SARTI, M., SCOTT, R.W., AND LI, X.H., 2005, Upper Cretaceous oceanic red beds in southern Tibet: a major change from anoxic to oxic, deep-sea environments: Cretaceous Research, v. 26, p. 21–32.

WEDEPOHL, K.H., 1971, Environmental influences on the chemical composition of shales and clays: *in* Ahrens, L.H., Press, F., Runcorn, S.K., and Urey, H.C., eds., Physics and Chemistry of the Earth: Oxford, U.K., Pergamon, 8, p. 305–333.

WORTMANN, U.G., HESSE, B., AND ZACHER, W., 1999, Major-element analysis of cyclic black shales: Paleoceanographic implications for the Early Cretaceous deep western Tethys: Paleoceanography, v. 14, p. 525–541.

ZIABREV, S.V., AITCHISON, J.C., ABRAJEVITCH, A.V., BADENGZHU, DAVIS, A.M., AND LUO, L., 2003, Precise radiolarian age constraints on the timing of ophiolite generation and sedimentation in the Dazhuqu terrane, Yarlung–Tsangpo suture zone, Tibet: Geological Society of London, Journal, v. 160, p. 591–599.

ZOU, Y.R., KONG, F., PENG, P.A., HU, X., AND WANG, C., 2005, Organic geochemical characterization of Upper Cretaceous oxic oceanic sediments in Tibet, China: A preliminary study: Cretaceous Research, v. 26, p. 65–71.

APPENDIX 1.—CORB distribution in continental outcrops. One sedimentary basin or tectonic zone is counted as 1.

Site No.	Country	Basin or tectonic zone	CC zones	Sediments*	Sources
1	Armenia	Lesser Caucasus	13–16	A1	Tur, 2002
2	Albania	Crasta–Cukali zone	9	A2	Robertson and Shallo, 2000
3	Austria	Helvetic Units	12, 14/15	A1	Wagreich et al., this volume
4	Austria	Ultrahelvetic, Upper Austria	11–18	A1, A2	Wagreich et al., this volume
5	Austria	Gresten Klippen Zone	9, 11–24	A2, A3	Widder, 1988
6	Austria	Rhenodanubian Flysch, Salzburg and Laab Nappem	9, 13–19, 21–22	A3	Wagreich et al., this volume;Wagreich, 2002
7	Austria	NCA Gosau Group and lower nappes	2–3, 7–8, 13, 16–26	A1, A2, A3	Wagreich et al., this volume;Wagreich and Krenmayr, 2005
8	Bulgaria	Central Srednogorie Zone	15–19	A1	Stoykov and Pavlishina, 2004
9	China	Tibet Tethys Himalaya, Chuangde Fm	16–22	A1, A3	Wan et al., 2005
10	Costa Rica	NW Costa Rica	? 15–23	A1	Kenneth Flores Reyes, personal communication, 2003
11	Czech Republic	Magura Nappes, Kaumberg Fm	10–23	A3	Svabnicka, 2003
12	Czech Republic	Bílé Karpaty Unit, Puchov Marl	22–25	A2, A3	Svabnicka, 2003
13	Czech Republic	Silesian Unit, Mazák Fm	10–14/15	A3	Skupien et al., this volume
14	Georgia	Cis–Caucasia	13–17	A1	Scherbinia, 2002
15	Georgia	Greater Caucasus	13–19	A1	Gambashidze, 2002
16	Germany	Rhenodanubian Flysch (Bavaria)	9, 14–18, 21–22	A3	Wagreich et al., this volume
17	Germany	Kirchrode II	8	A2	Fenner et al., 2004
18	Greece	Pindos Zone	9–17	A1, A2, A3, A5	Neumann and Wagreich, this volume
19	Greenland	NE Greenland	2–3	A2, A3	Alsen, P., and Surlyk, F., 2004
20	Hungary	Szolnok Flysch Zone, Vekeny Marl	11–13	A2	Balla and Bodrogi, 1993
21	India	Ladakh Himalaya, Lamayuru Fm	18–23	A1	Robertson and Sharp, 1998
22	India	Zanskar himalaya, Fatu La Fm	9, 11–19	A1	Premoli Silva et al., 1991
23	India	Cauvery Basin	16–17	A3	Govindan, 2006
24	Italy	Umbria–Marche basin/Marne a Fucoidi, Scaglia Bianica, Scaglia Rossa	7–26	A1, A2, A3, A5	Premoli Silva and Sliter, 1994; Hu et al., 2006
25	Italy	Southern Alps/Scaglia Rossa	11–26	A1, A2	Hu et al., 2005
26	Italy	Southern Alps, Cismon Core	5, 8	A1, A2,A5	Erba et al., 1999
27	New Zealand	North Island	10–14/15	A3	Hikuroa and Crampton, this volume
28	Poland	Pieniny Klippen Belt, Jaworki Fm and Czorsztyn Ridge	9–23	A1, A2,A3	Bak, 2002

APPENDIX 1 (continued).—CORB distribution in continental outcrops.

Site No.	Country	Basin or tectonic zone	CC zones	Sediments*	Sources
29	Poland	Skole Basin	11, 14/15, 20, 23/24	A3	Bak, 2002
30	Poland	Magura Basin, Malinowa shale Fm	11–24	A3	Bak, 2002
31	Poland	Subsilesian Basin, Weglowka Marl	12–26	A3	Bak, 2002
32	Romania	Outer Dacides and Moldavides, Gura belie Fm	21–26	A2	Melinte and Jipa, 2005
33	Romania	Inner and Outer Moldavides	9–13	A3	Melinte et al., this volume
34	Russia,Dagestan	Eastern Caucasus	12–16	A1	Scherbinia, 2002
35	Serbia	Vojvodina	22–24	A1	Dulic et al., 2006
36	Slovakia	Tatric units, Kosariska Formation	18–22	A2	Michalik et al., 2002
37	Slovakia	Pieniny Klippen Belt, Puchov Fm	11–19	A2	Michalik et al., 2002
38	Spain	Subbetic Zone, Capas Rojas	9–26	A1, A2	Vera and Molina, 1999
39	Switzerland	Romandes Prealps/Roter Sattel	9–26	A1, A2	Strasser et al., 2001
40	Turkey	Pontides/Unaz Fm	10–18	A1, A2	Tüysüz et al., 2003
41	Turkey	Sakarya Zone	11–13, 17–18	A1,A2	Yilmaz and Altiner, 2006
42	Turkey	Taurides	11–26	A1	Yilmaz et al., 2006
43	Turkey	Arabian Platform	11–20	A1	Yilmaz et al., 2006
44	Turkmenistan	N Caucasus	7–8, 12–24	A1	Tur, 2002
45	Turkmenistan	NE Caucasus	12–17	A1	Tur and Wagreich, 2005
46	Turkmenistan	Western Kopet Dag	12–16	A1, A2	Scherbinia, 2002
47	U.S.A	California	8–9	A3	Bubik, 2006
48	Ukraine	E Carpathians, Puchov Fm	11–24	A2	Scherbinia, 2002
49	Ukraine	Crimea	13–15	A1, A2	Scherbinia, 2002
50	U.K.	NE England, Hunstanton Fm	8–9	A1, A2	Mitchell, 1995
51	Germany	Rotpläner	10–14–15	B4	Wiese, this volume
52	Jordan	Eastern Levant carbonate platform	11	B1	Wendler et al., this volume
53	Tunisia	Central Tunisia Platform	10–13	B1	Abdallah et al., 2006

*A (Hemi)pelagic, deep water; B Shallow water; 1 Limestone; 2 Marl; 3 Shale; 4 Chalk; 5 Chert

References for Appendix 1.

ABDALLAH, H., SASSI, A.B, AND SASSI, S., 2006, the middle Cenomanian and Turonian red beds in central Tunisia: preliminary investigations, *in* Hu, X., Wang, Y., and Huang, Y., eds., International Symposium on Cretaceous Major Geological Events and Earth System—Workshop on Cretaceous Oceanic Red Beds (IGCP 463 and 494), Program and Abstracts: China University of Geosciences, Beijing, China, p. 1–3.

ALSEN, P., AND SURLYK, F., 2004, Deep marine red beds of the Valanginian–Hauterivian (Lower Cretaceous) of East Greenland: Palaeo-oceanographic implications (abstract): 32nd International Geological Congress, Session T29.10, Abstracts.

BAK, K., 2002, Cretaceous oceanic red beds in southern Poland, *in* Hu, X., and Sarti, M., eds., Cretaceous Oceanic Red Beds (CORBs) in an Apennines–Alps–Carpathians Transect: Field Guidebook for Inaugural Workshop of IGCP 463, Ancona, Italy, p. 73–115.

BALLA, Z., AND BODROGI, I., 1993, The 'Vékény Marl Formation' of Hungary: Cretaceous Research, v. 14, p. 431–448.

Bubik, M., 2006, Cretaceous oceanic red beds in the Eastern Pacific Province: Orchard Peak section, California (abstract), *in* Hu, X., Wang, Y., and Huang, Y., eds., International Symposium on Cretaceous Major Geological Events and Earth System—Workshop on Cretaceous Oceanic Red Beds (IGCP 463 and 494), Program and Abstracts: China University of Geosciences, Beijing, China, p. 29.

Dulic, I., Wagreich, M., and Jovanovic, R., 2006, 1st International Workshop Mesozoic Sediments of Carpatho-Balkanides and Dinarides, Abstracts and Field Guide, 72 p. (NIS Naftagas, Novi Sad).

Erba, E., Channell, J.E.T., Claps, M., Jones, C., Larson, R.L., Opdyke, B., Premoli Silva, I., Riva, A., Salvini, G., and Torricelli, S., 1999, Integrated stratigraphy of the Cismon Apti-core (Southern Alps, Italy): a 'reference section' for the Barremian–Aptian interval at low latitudes: Journal of Foraminiferal Research, v. 29, p. 371 –391.

Fenner, J.M., Hild, E., Brumsack, H.J., Benesch, M., and Heydemann, A., 2004, Middle Albian red beds in the research borehole Kirchrode II (abstract), *in* 32nd International Geological Congress, Florence 2004, Scientific Sessions, abstracts (part 1), p. 574.

Gambashidze, R.A., 2002, The Upper Cretaceous oceanic red beds of Georgia (abstract): Inaugural Workshop of IGCP 463, Ancona, Italy, Program and Abstracts, p. 5.

Govindan, A., 2006, Implications of oceanic anoxic events, regional source rock distribution and marine red beds in the Cretaceous sequence in Cauvery Basin, South India: towards paleoceanographic and paleoclimatic inferences (abstract), *in* Hu, X., Wang, Y., and Huang, Y., eds., International Symposium on Cretaceous Major Geological Events and Earth System—Workshop on Cretaceous Oceanic Red Beds (IGCP 463 and 494), Program and Abstracts: China University of Geosciences, Beijing, China, p. 41–42.

Hu, X., Jansa, L., Wang, C., Sarti, M., Bak, K., Wagreich, M., Michalik, J., and Soták, J., 2005, Upper Cretaceous oceanic red beds (CORBs) in the Tethys: occurrences, lithofacies, age, and environments: Cretaceous Research, v. 26, p. 3–20.

Hu, X., Jansa, L., and Sarti, M., 2006, Mid-Cretaceous oceanic red beds in the Umbria–Marche Basin, central Italy: Constraints on paleoceanography and paleoclimate: Palaeogeography, Palaeoclimatology, Palaeoecology, v. 233, p. 163–186.

Melinte, M.C., and Jipa, D.C., 2005, Campanian–Maastrichtian marine red beds in Romania: biostratigraphic and genetic significance: Cretaceous Research, v. 26, p. 49–56.

Michalik, J., Soták, J., and Salaj, J., 2002, Cretaceous Oceanic Red Beds in the westernmost Carpathians in Slovakia, *in* Hu, X., and Sarti, M., eds., Cretaceous Oceanic Red Beds (CORBs) in an Apennines–Alps–Carpathians Transect: Field Guidebook for Inaugural Workshop of IGCP 463, Ancona, Italy, p. 47–72.

Mitchell, S.F., 1995, Lithostratigraphy and biostratigraphy of the Hunstanton Formation (Red Chalk, Cretaceous) succession at Speeton, North Yorkshire, England: Yorkshire Geological Society, Proceedings, v. 50, p. 285–303.

Premoli Silva, I., and Sliter, W.V., 1994, Cretaceous planktonic foraminiferal biostratigraphy and evolutionary trends from the Bottaccione section, Gubbio, Italy: Paleontographica Italica, v. 82, p. 1–89.

Premoli Silva, I., Garzanti, E., and Gaetani, M., 1991, Stratigraphy of the Chikkim and Fatu La Formations in the Zangla and Zumlung Units (Zanskar Range, India) with comparisons to the Thakkhola region (central Nepal): Mid-Cretaceous evolution of the Indian passive margin: Rivista Italiana di Paleontologia e Stratigrafia, v. 97, p. 511–564.

Robertson, A., and Shallo, M., 2000, Mesozoic–Tertiary tectonic evolution of Albania in its regional Eastern Mediterranean context: Tectonophysics, v. 316, p. 197–254.

Robertson, A., and Sharp, I., 1998, Mesozoic deep-water slope/rise sedimentation and volcanism along the North Indian passive margin: evidence from the Karamba Complex, Indus suture zone (Western Ladakh Himalaya): Journal of Asian Earth Sciences, v. 16, p. 195–215.

Scherbinina, E.A., 2002, The Upper Cretaceous red beds of the Northeastern Peri-Tethys (abstract): Inaugural Workshop of IGCP 463, Ancona, Italy, Program and Abstracts, p. 26–27.

Stoykov, S., and Pavlishina, P., 2004, Santonian–Campanian red beds in the Northern part of the Central Srednogorie zone, Bulgaria (abstract), *in* Melinte M.C., Brustur, T., Jipa, D., and Szobotka, S., eds., IGCP 463 and 494 Workshop, Romania, August 15–18, 2004, Abstract volume, p. 26–28

Strasser, A., Caron, M., and Gjermeni, M., 2001, The Aptian, Albian and Cenomanian of Roter Sattel, Romandes Prealps, Switzerland: a high-resolution record of oceanographic changes: Cretaceous Research, v. 22, p. 173–199.

Svabenicka, L., 2003, Upper Cretaceous oceanic red beds in the Outer West Carpathians, Margura Group of Nappes, Czech Republic (abstract), *in* Tuysuz, O., and Yikilmaz, B., eds., Upper Cretaceous Oceanic Red Beds Workshop: Bartin, Turkey, August 18–23, 2003, Program and Abstracts, p. 25.

Tur, N.A., 2002, Red hemipelagic sequences in the Upper Cretaceous of north Tethys (N. Caucasus, Tuarkyr and W. Kopeth-Dag) (abstract): Inaugural Workshop of IGCP 463, Ancona, Italy, Program and Abstracts, p. 29.

Tur, N., and Wagreich, M., 2005, Bio- and isotope stratigraphy of Late Cretaceous oceanic red beds in the NE Caucasus, *in* Godet, A., Mort, H., Linder, P., and Bodin, S., eds.: 7th International Workshop on Cretaceous, September 5–9, 2005, Scientific Program and Abstracts, p. 214–215.

Tüysüz, O., 2002, Upper Cretaceous red pelagic limestones in the Pontides, northern Turkey and their significance on the geological evolution of Black Sea (abstract): Inaugural Workshop of IGCP 463, Ancona, Italy, Program and Abstracts, p. 30.

Vera, J.A., and Molina, J.M., 1999, La Formación Capas Rojas: Caracterización y Genesis: Estudios Geológicos, v. 55, p. 45–66.

Wagreich, M., 2002, Cretaceous Oceanic Red Beds in Austria Alps, *in* Hu, X., and Sarti, M., eds., Cretaceous Oceanic Red Beds (CORBs) in an Apennines–Alps–Carpathians Transect: Field Guidebook for Inaugural Workshop of IGCP 463, Ancona, Italy, p. 30–46.

Wagreich, M., and Krenmayr, H.-G., 2005, Upper Cretaceous oceanic red beds (CORBs) in the Northern Calcareous Alps, (Nierental Formation, Austria): slope topography and clastic input as primary controlling factors: Cretaceous Research, v. 26, p. 57–64.

Wan, X., Lamolda, M.A., Si, J., Li, G., 2005, Foraminiferal stratigraphy of Cretaceous red beds in southern Tibet: Cretaceous Research, v. 26, p. 43–48.

Widder, R., 1988, Zur Stratigraphie, Fazies und Tektonik der Grestener Klippenzone zwischen Maria Neustift und Pechgraben/O.Ö: Gesellschaft der Geologie und Bergbaustudenten Österreichs, Mitteilungen, v. 34/35, p. 79–133.

Yilmaz, I.O., and Altiner, D., 2006, Anoxic event and red beds across the Cenomanian/Turonian boundary (NW Turkey) (abstract), *in* Hu, X., Wang, Y., and Huang, Y., eds., International Symposium on Cretaceous Major Geological Events and Earth System—Workshop on Cretaceous Oceanic Red Beds (IGCP 463 and 494), Program and Abstracts: China University of Geosciences, Beijing, China, p. 106.

Yilmaz, I. O., Tüysüz, O., Altiner, D., and Genç, S.C., 2006, Tectonic setting and paleoceanographic implications of Upper Cretaceous red beds in Turkey (abstract), *in* Hu, X., Wang, Y., and Huang, Y., eds., International Symposium on Cretaceous Major Geological Events and Earth System—Workshop on Cretaceous Oceanic Red Beds (IGCP 463 and 494), Program and Abstracts: China University of Geosciences, Beijing, China, p. 105.

APPENDIX 2.—CORB distribution in the oceanic DSDP and ODP sites.

Ocean	Leg	Site	Geographic position	Age	Lithology*	Color	Source
North Atlantic	1	7a	-----	11–26	A3	yellowish red	Ewing, M., et al., 1969, DSDP Initial Reports, v. 1
North Atlantic	2	9a	-----	16–23	A3	yellowish red	Peterson, M.N.A., et al., 1970, DSDP Initial Reports, v. 2
North Atlantic	10	86	Gulf of Mexico	8–9	B7	yellowish brown	Worzel, et al., 1973. DSDP Initial Reports, v. 10
North Atlantic	10	95	Gulf of Mexico	8–9	B7	yellowish brown	Worzel, et al., 1973. DSDP Initial Reports, v. 10
North Atlantic	11	105	Caribbean	9–26	A3	reddish brown, yellow orange	Charles, et al., 1972. DSDP Initial Reports, v. 11
North Atlantic	14	136	160 km North Madeira	7–16	A3	brown, reddish brown, red	Hayes, et al., 1972. DSDP Initial Reports, v. 14
North Atlantic	14	137	100 km west Cap Blanc, Africa	9–10, 17–26	A2, A3, A4	brown, varicolored	Hayes, et al., 1972. DSDP Initial Reports, v. 14
North Atlantic	14	138	100 km west Cap Blanc, Africa	17–23	A3	reddish brown	Hayes, et al., 1972. DSDP Initial Reports, v. 14
North Atlantic	15	150	Venezuelan Basin, Caribbean	11–15	A2, A4	yellowish brown, varicolored	Edgar, et al., 1973. DSDP Initial Reports, v. 15
North Atlantic	43	382	Nashville Seamount	17–23	A2, A3	brown, grayish brown, reddish brown	Tucholke, et al., 1979. DSDP Initial Reports, v. 43
North Atlantic	43	384	Newfoundland Ridge	24–26	A4	very pale yellow	Tucholke, et al., 1979. DSDP Initial Reports, v. 43
North Atlantic	43	385	Volgel Seamount	11–25	A3	yellowish red	Tucholke, et al., 1979. DSDP Initial Reports, v. 43
North Atlantic	43	386	Bermuda	10–26	A3	red	Tucholke, et al., 1979. DSDP Initial Reports, v. 43
North Atlantic	43	387	Bermuda Rise	23	A3	red	Tucholke, et al., 1979. DSDP Initial Reports, v. 43
North Atlantic	44	391	Blake–Bahama Basin	9–26	A3	varicolored. yellowish brown, dark brown, yellowish red, dark greenish brown	Benson, et al., 1978. DSDP Initial Reports, v. 44
North Atlantic	47	398	Vigo Seamount	11–26	A3	red, yellow brown	Ryan, et al., 1979. DSDP Initial Reports, v. 47
North Atlantic	48	400	Biscay	22–25	A4	reddish yellow	Montadert, et al., 1979. DSDP Initial Reports, v. 48
North Atlantic	48	401	Meriadzek Terrace	22–25	A4	grayish orange	Montadert, et al., 1979. DSDP Initial Reports, v. 48
North Atlantic	51–53	417	Bermuda Rise	14–26	A3	varicolored. Dark and light yellow brown. Cyclic pale green and yellow brown	Donnelly, et al., 1979. DSDP Initial Reports, v. 51, 52, 53
North Atlantic	51–53	418	Bermuda Rise	14–26	A2, A3, A4	dark brown, yellow brown, pale orange, dark red brown	Donnelly, et al., 1979. DSDP Initial Reports, v. 51, 52, 53
North Atlantic	48	534	Blake–Bahama Basin	7–8, 23–24	A3	yellowish brown, dark brown, yellowish red, dark greenish brown	Sheridan R.E., et al., 1983, DSDP Initial Reports, v. 48
North Atlantic	80	548	Goban Spur	21–26	A4	varicolored. Moderate orange pink, grayish orange pink.	De Graciansky, et al., 1985. DSDP Initial Reports, v. 80
North Atlantic	80	549	Goban Spur	11–26	A4	light brown	De Graciansky, et al., 1985. DSDP Initial Reports, v. 80
North Atlantic	80	550	Goban Spur	9	A3	reddish and brownish	De Graciansky, et al., 1985. DSDP Initial Reports, v. 80
North Atlantic	93	603	Hatteras Abyssal Plain	11–17	A3	reddish brown,	Van Hinte, et al., 1987. DSDP Initial Reports, v. 93
North Atlantic	103	640	Calicia Margin	7–8	A3	brown, yellowish brown	Boillot, et al., 1987. ODP Initial Reports, v. 103
North Atlantic	103	641	Calicia Margin	9–25	A3	brown, grayish brown	Boillot, et al., 1987. ODP Initial Reports, v. 103
North Atlantic	171	1049	Blake Nose	7–8	A3, A4	cyclic greenish and reddish	Kroon, et al., 1998. ODP Initial Reports, v. 171
North Atlantic	171	1050	Blake Nose	10–12	A4	red	Kroon, et al., 1998. ODP Initial Reports, v. 171
North Atlantic	173	1070	Vigo Seamount	7–25	A3	varicolored: medium brown, light brown, moderate yellowish orange	Whitmarsh, et al., 1998. ODP Initial Reports, v. 173
South Atlantic	3	20	western flank of the Mid-Atlantic Ridge	22–26	A2	very pale brown, pink	Maxwell, et al., 1970. DSDP Initial Reports, v. 3
South Atlantic	3	21	Rio Grande Rise	22–26	A2	very pale brown, pink	Maxwell, et al., 1970. DSDP Initial Reports, v. 3
South Atlantic	36	328	Malvinas outer Basin	12–26	A3	cyclic red and brown	Barker, et al., 1976. DSDP Initial Reports, v. 36
South Atlantic	36	330	Falkland Plateau	8	A3	gryish orange, light brown	Barker, et al., 1976. DSDP Initial Reports, v. 36
South Atlantic	39	354	Ceara Rise	24–26	A4	pale red	Perch-Nielsen, et al., 1977. DSDP Initial Reports, v. 39
South Atlantic	39	355	Brazil Basin	17–25	A2	brown	Perch-Nielsen, et al., 1977. DSDP Initial Reports, v. 39
South Atlantic	39	356	Sao Paulo Plateau	17–22	A4	pale red	Perch-Nielsen, et al., 1977. DSDP Initial Reports, v. 39
South Atlantic	39	357	Rio Grande Rise	23–26	A1, A4	grayish orange, pale yellowish brown	Perch-Nielsen, et al., 1977. DSDP Initial Reports, v. 39
South Atlantic	39	358	Argentine Basin	23–26	A3, A4	red brown	Perch-Nielsen, et al., 1977. DSDP Initial Reports, v. 39
South Atlantic	40	361	Cape Agulhas	7–25	A3	alteration of red and grayish	Bolli, et al. 1978. DSDP Initial Reports, v. 40

References for Appendix 2.

Note: Many references were from the ODP or DSDP initial reports. The authors of the descriptions of each site are often Shipboard Scientific Party, which means there are too many coauthors for the descriptions of each site. Moreover, because of the large number of references of this kind (more than 70), it would be too hard to identify them if we just list the Shipboard Scientific Party into different references as the authors. Therefore, we list the first three of them and "et al." for the others into the references according to the note in the reports, instead of listing all of names or just Shipboard Scientific Party.

ANDREWS, J.E., EADE, J.V., HOLDSWORTH, B.K., ET AL., 1975a, Site 288, *in* Andrews, J.E., Packham, G., et al., eds., Initial Reports of the Deep Sea Drilling Project, v. 30: Washington, U.S. Government Printing Office, p. 175–230.

ANDREWS, J.E., EADE, J.V., HOLDSWORTH, B.K., ET AL., 1975b, Site 289, *in* Andrews, J.E., Packham, G., et al., eds., Initial Reports of the Deep Sea Drilling Project, v. 30: Washington, U.S. Government Printing Office, p. 231–398.

BARKER, P., DALZIEL, I.W.D., DINKELMAN, M.G., ET AL., 1976a, Site 328, *in* Barker, P., Dalziel, I.W.D., et al., eds., Initial Reports of the Deep Sea Drilling Project, v. 36: Washington: U.S. Government Printing Office, p. 87–142.

BARKER, P., DALZIEL, I.W.D., DINKELMAN, M.G., ET AL., 1976b, Site 330, *in* Barker, P., Dalziel, I.W.D., et al., eds., Initial Reports of the Deep Sea Drilling Project, v. 36: Washington: U.S. Government Printing Office, p. 207–258.

BENSON, W.E., SHERIDAN, R.E., ENOS, P., ET AL., 1978a, Sites 389 and 390: North Rim of Blake Nose, *in* Benson, W.E., Sheridan, R.E., et al., eds., Initial Reports of the Deep Sea Drilling Project, v. 44: Washington: U.S. Government Printing Office, p. 69–152.

BENSON, W.E., SHERIDAN, R.E., ENOS, P., ET AL., 1978b, Sites 391: Blake–Bahama Basin, *in* Benson, W.E., Sheridan, R.E., et al., eds., Initial Reports of the Deep Sea Drilling Project, v. 44: Washington: U.S. Government Printing Office, p. 159–336.

BOILLOT, G., WINTERER, E.L., MEYER, A.W., ET AL., 1987a, Site 640, *in* Boillot, G., Winterer, E.L., Meyer, A.W., et al., eds., Initial Reports (part A) of the Ocean Drilling Program, v. 103, p. 533–570.

BOILLOT, G., WINTERER, E.L., MEYER, A.W., ET AL., 1987b, Site 641, *in* Boillot, G., Winterer, E.L., Meyer, A.W., et al., eds., Initial Reports (part A) of the Ocean Drilling Program, v. 103. 571–652.

BOLLI, H.M., RYAN, W.B.F., FORESMAN, J.B., ET AL., 1978a, Cape basin continental rise—sites 360 and 361, *in* Bolli, H.M., Ryan, W.B.F., et al., eds., Initial Reports of the Deep Sea Drilling Project, v. 40: Washington: U.S. Government Printing Office, p. 29–182.

BOLLI, H.M., RYAN, W.B.F., FORESMAN, J.B., ET AL., 1978b, Angola continental margins—sites 364 and 365, *in* Bolli, H.M., Ryan, W.B.F., et al., eds.,

APPENDIX 2 (continued).

Ocean	Leg	Site	Geographic position	Age	Lithology*	Color	Source
South Atlantic	40	364	Angola Basin	9–26	A3, A4	light brown, brown, reddish brown	Bolli, et al. 1978. DSDP Initial Reports, v. 40
South Atlantic	41	367	Cape Verde Basin	7–8, 16–23	A3	dark reddish brown intercalated with dark gray	Lancelot, et al., 1977. DSDP Initial Reports, v. 41
South Atlantic	71	511	Falkland Plateau	8–13	A3, A4	reddish brown	Ludwig, et al., 1983. DSDP Initial Reports, v. 71
South Atlantic	73	524	Cape Basin	25–26	A3	reddish brown	Hsü, et al., 1984. DSDP Initial Reports, v. 73
South Atlantic	74	525	Walviss Ridge	25–26	A4	pinkish gray, light brown, yellowish brown	Moore, et al., 1984. DSDP Initial Reports, v. 74
South Atlantic	74	527	Walviss Ridge	25–26	A4	reddish yellow, pink, pale brown	Moore, et al., 1984. DSDP Initial Reports, v. 74
South Atlantic	74	528	Walviss Ridge	25–26	A4	reddish brown	Moore, et al., 1984. DSDP Initial Reports, v. 74
South Atlantic	207	1258	Demerara Rise	26	A4	yellowish red, yellowish brown	Erbacher, et al., 2004. ODP Initial Reports, v. 207
South Atlantic	207	1259	Demerara Rise	26	A4	reddish brown, reddish	Erbacher, et al., 2004. ODP Initial Reports, v. 207
South Atlantic	207	1260	Demerara Rise	26	A4	reddish brown, reddish	Erbacher, et al., 2004. ODP Initial Reports, v. 207
South Atlantic	208	1262	Angola Basin	26	A2, A3	reddish brown	Zachos, et al., 2004. ODP Initial Reports, v. 208
South Atlantic	208	1267	Angola Basin	26	A2, A3	light reddish brown, brown	Zachos, et al., 2004. ODP Initial Reports, v. 208
Pacific	16	163	central equatorial Pacific	17–25	A4	very pale orange, very pale pinkish orange	Van Andel, et al., 1973. DSDP Initial Reports, v. 16
Pacific	17	164	Central Basin	8–22	A4, A5	brown	Winterer, et al., 1973. DSDP Initial Reports, v. 17
Pacific	17	167	Central Basin	8–10, 13–14, 17–19	A1	grayish orange pink, light brown to dark reddish brown	Winterer, et al., 1973. DSDP Initial Reports, v. 17
Pacific	17	169	Central Basin	9–11, 21–26	A3	yellow brown, brown, pink	Winterer, et al., 1973. DSDP Initial Reports, v. 17
Pacific	17	170	Central Basin	9–25	A1, A3, A4	brown, pink	Winterer, et al., 1973. DSDP Initial Reports, v. 17
Pacific	19	192	Meiji Guyot	25–26	A1, A4	moderate to light brown	Scholl, et al., 1973. DSDP Initial Reports, v. 19
Pacific	20	196	east of Mariana Trench	17–23	A3	red	Heezen, et al., 1973. DSDP Initial Reports, v. 20
Pacific	30	288	Ontong Java Plateau	9–10	A1	pink, pinkish gray, light reddish brown	Andrews, et al., 1975. DSDP Initial Reports, v. 30
Pacific	30	289	Ontong Java Plateau	7, 18–21	A1	pinkish gray, orange brown, reddish brown	Andrews, et al., 1975. DSDP Initial Reports, v. 30
Pacific	32	310	Hess Rise	17–25	A2	very pale orange, dark or moderate yellowish orange,	Larson, et al., 1975. DSDP Initial Reports, v. 32
Pacific	32	313	mid-Pacific Mountains	25–26	A1	pale brown	Larson, et al., 1975. DSDP Initial Reports, v. 32
Pacific	33	315	Line Island	12–17, 22–26	A1, A3	dark orange brown, pale orange, light brown	Schlanger, et al., 1976. DSDP Initial Reports, v. 33
Pacific	33	316	Line Island	12–17, 22–26	A1, A3	brown, dusky brown	Schlanger, et al., 1976. DSDP Initial Reports, v. 33
Pacific	62	463	mid-Pacific Mountains	7–8	A1	cyclic, pink, green, brown and white	Thiede, et al., 1981. DSDP Initial Reports, v. 62
Pacific	62	464	Hess Rise	10–24	A3, A5	brown	Thiede, et al., 1981. DSDP Initial Reports, v. 62
Pacific	86	576	Between Shatsky Rise and the Emperor Seamounts	17–23	A2, A3	dark brown, pale brown	Heath, et al., 1985. DSDP Initial Reports, v. 86
Pacific	129	801	Pigafetta Basin	19–26	A3	brown	Lancelot, et al., 1990. ODP Initial Reports, v. 129
Pacific	181	1124	Rekohu Drift	25–26	A3	brown, pink	Carter, et al., 1999. ODP Initial Reports, v. 181
Pacific	192	1183	Ontong Java Plateau	7–9,13–16	A1	pinkish white, reddish, pink, reddish brown	Mahoney, et al., 2001. ODP Initial Reports, v. 192
Pacific	198	1207	Shatsky transect	11–21	A1, A4, A2, A5	dusky yellow brown, very pale orange, grayish orange	Bralower, et al., 2002. ODP Initial Reports, v. 198
Indian	22	211	Wharton Basin	17–25	A2, A3	varicolored, gray, cream and red	Borch, et al., 1974. DSDP Initial Reports, v. 22
Indian	22	212	Wharton Basin	25–26	A4	gryayish orange pink	Borch, et al., 1974. DSDP Initial Reports, v. 22
Indian	22	217	Wharton Basin	25–26	A4	grayish orange pink, light brown	Borch, et al., 1974. DSDP Initial Reports, v. 22
Indian	25	249	Mozambique Ridge	23–26	A4	brown	Simpson, et al., 1974. DSDP Initial Reports, v. 25
Indian	27	259	Wharton Basin	13–25	A3	yellowish brown, light brown	Veevers, et al., 1974. DSDP Initial Reports, v. 27
Indian	27	260	Wharton Basin	13–25	A3, A2	moderate brown, moderate orange pink	Veevers, et al., 1974. DSDP Initial Reports, v. 27
Indian	27	261	Wharton Basin	1–2, 14–25	A3	dark yellowish brown, moderate brown	Veevers, et al., 1974. DSDP Initial Reports, v. 27
Indian	122	762	Exmouth Plateau	8–15,17–24	A3, A4	cyclic red brown, light red brown, white or light green gray; cyclic brown, light brown, white or light green gray	Haq, et al., 1990. ODP Initial Reports, v. 122
Indian	183	1136	Kerguelen Plateau	8–9,18–21	A2, B6	brown; very light brown	Coffin, et al., 2000. ODP Initial Reports, v. 183

Initial Reports of the Deep Sea Drilling Project, v. 40: Washington: U.S. Government Printing Office, p. 357–456.

BORCH, C.C. VON DER, SCLATER, J.G., GARTNER, S. JR., ET AL., 1974a, Site 211, *in* Borch, C.C. von der, Sclater, J.G., et al., eds., Initial Reports of the Deep Sea Drilling Project, v. 22: Washington: U.S. Government Printing Office, p. 13–36.

BORCH, C.C. VON DER, SCLATER, J.G., GARTNER, S. JR., ET AL., 1974b, Site 212, *in* von der Borch, C.C., Sclater, J.G., et al., eds., Initial Reports of the Deep Sea Drilling Project, v. 22: Washington: U.S. Government Printing Office, p. 37–84.

BORCH, C.C. VON DER, SCLATER, J.G., GARTNER, S. JR., ET AL., 1974c, Site 217, *in* von der Borch, C.C., Sclater, J.G., et al., eds., Initial Reports of the Deep Sea Drilling Project, v. 22: Washington: U.S. Government Printing Office, p. 267–324.

BRALOWER, T.J., PREMOLI SILVA, I., MALONE, M.J., ET AL., 2002. Leg 198 summary, *in* Bralower, T.J., Premoli Silva, I., Malone, M.J., et al., eds., Proceedings of the Ocean Drilling Project, Initial Reports, v. 198. College Station TX (Ocean Drilling Program), p. 1–148.

CARTER, R.M., MCCAVE, I.N., RICHTER, C., ET AL., 1999, Leg 181 summary: Southwest Pacific paleoceanography, *in* Carter, R.M., McCave, I.N., Richter, C., et al., eds., Proceedings of the Ocean Drilling Project, Initial Reports, v. 181: College Station TX (Ocean Drilling Program), p. 1–80.

HOLLISTER, C.D., EWING, J.I., HABIB, D., ET AL., 1972, Site 105: Lower continental rise hills, *in* Hollister, C.D., Ewing, J.I., et al., eds., Initial Reports of the Deep Sea Drilling Project, v. 11: Washington, U.S. Government Printing Office, p. 1—1077.

COFFIN, M.F., FREY, F.A., WALLACE, P.J., ET AL., 2000. Leg 183 summary: Kerguelen Plateau–Broken Ridge—A large igneous province, *in* Coffin, M.F., Frey, F.A., Wallace, P.J., et al., eds., Proceedings of the Ocean Drilling Project, Initial Reports, v. 183: College Station TX (Ocean Drilling Program), p. 1–101.

DE GRACIANSKY, P.C., POAG, C.W., CUNNINGHAM, R., ET AL., 1985a, Site 548, *in* DeGraciansky, P.C., Poag, C.W., et al., eds., Initial Reports of the Deep Sea Drilling Project, v. 80: Washington, U.S. Government Printing Office, p. 33–122.

DE GRACIANSKY, P.C., POAG, C.W., CUNNINGHAM, R., ET AL., 1985b, Site 549, *in* DeGraciansky, P.C., Poag, C.W., et al., eds., Initial Reports of the Deep Sea Drilling Project, v. 80: Washington, U.S. Government Printing Office, p. 123–250.

DE GRACIANSKY, P.C., POAG, C.W., CUNNINGHAM, R., ET AL., 1985c, Site 550, *in* DeGraciansky, P.C., Poag, C.W., et al., eds., Initial Reports of the Deep Sea Drilling Project, v. 80: Washington, U.S. Government Printing Office, p. 251–356.

DONNELLY, T.W., FRANCHETEAU, J., BLEIL, U., ET AL., 1979a, Site 417, *in* Donnelly, T.W., Francheteau, J., Bryan, W., et al., eds., Initial Reports

of the Deep Sea Drilling Project, v. 51, 52, 53, Part 1: Washington, U.S. Government Printing Office, p. 23–350.

Donnelly, T.W., Francheteau, J., Bleil, U., et al., 1979b, Site 418, *in* Donnelly, T.W., Francheteau, J., Bryan, W., et al., eds., Initial Reports of the Deep Sea Drilling Project, v. 51, 52, 53, Part 1: Washington, U.S. Government Printing Office, p. 351–626.

Edgar, N.T., Saunders, J.B., Bolli, H.M., et al., 1973, Site 150, *in* Edgar, N.T., Saunders, J.B., et al., eds., Initial Reports of the Deep Sea Drilling Project, v. 15: Washington, U.S. Government Printing Office, p. 277–308.

Erbacher, J., Mosher, D.C., Malone, M.J., et al., 2004, Leg 207 summary, *in* Erbacher, J., Mosher, D.C., Malone, M.J., et al., eds., Proceedings of the Ocean Drilling Project, Initial Reports, v. 181: College Station, TX (Ocean Drilling Program), p. 1–89.

Ewing, M., Worzel, J.L., Beall, A.O., et al., 1969, Site 7, *in* Ewing, M., Worzel, J.L., et al., eds., Initial Reports of the Deep Sea Drilling Project, v. 1: Washington, U.S. Government Printing Office, p. 293–317.

Foreman, H. P., 1971, Cretaceous Radiolaria, Leg 7, DSDP, *in* Winterer, E. L., et al., eds., Initial Reports of the Deep Sea Drilling Project, 7: Washington (U. S. Government Printing Office), p. 1673–1693.

Haq, B.U., von Rad, U., O'Connell, S., et al., 1990, Site 762, *in* Haq, B.U., von Rad, U., O'Connell, S., et al., eds., Proceedings of the Ocean Drilling Program, Initial Reports, 122, College Station, TX (Ocean Drilling Program), p. 213–288.

Hayes, D.E., Pimm, A.C. Beckmann, J.P., et al., 1972a, site 136, *in* Hayes D. E., Pimm, A. C., et al., 1972, Initial Reports of the Deep Sea Drilling Project, v. 14: Washington, U.S. Government Printing Office, p. 975.

Hayes, D.E., Pimm, A.C. Beckmann, J.P., et al., 1972b, site 137, *in* Hayes D. E., Pimm, A. C., et al., eds., 1972, Initial Reports of the Deep Sea Drilling Project, v. 14: Washington, U.S. Government Printing Office, p. 975.

Hayes, D.E., Pimm, A.C. Beckmann, J.P., et al., 1972c, site 138, *in* Hayes D. E., Pimm, A. C., et al., eds., Initial Reports of the Deep Sea Drilling Project, v. 14: Washington, U.S. Government Printing Office, p. 975.

Heath, G.R., Burckle, L.H., Bleil, U., et al., 1985, Site 576, *in* Heath, G.R., Burckle, L.H., et al., eds., Initial Reports of the Deep Sea Drilling Project, v. 86: Washington, U.S. Government Printing Office, p. 51–90.

Heezen, B.C., Foreman, H.P., Hekel, Z.H., et al., 1973. Pliocene Volcanogenic sediments and Mesozoic chalks southeast of Japan: DSDP Site 196, *in* Heezen, B.C., MacGregor, I.D., et al., eds., Initial Reports of the Deep Sea Drilling Project, v. 14: Washington, U.S. Government Printing Office, p. 33–44.

Heirtzler, J.R., Veevers, J.J., Bolli, H.M., et al., 1974a, Site 259, *in* Veevers, J.J., Heirtzler, J.R., et al., eds., Initial Reports of the Deep Sea Drilling Project, v. 27: Washington, U.S. Government Printing Office, p. 15–88.

Heirtzler, J.R., Veevers, J.J., Bolli, H.M., et al., 1974b, Site 260, *in* Veevers, J.J., Heirtzler, J.R., et al., eds., Initial Reports of the Deep Sea Drilling Project, v. 27: Washington, U.S. Government Printing Office, p. 89–128.

Heirtzler, J.R., Veevers, J.J., Bolli, H.M., et al., 1974c, Site 261, *in* Veevers, J.J., Heirtzler, J.R., et al., eds., Initial Reports of the Deep Sea Drilling Project, v. 27: Washington, U.S. Government Printing Office, p. 129–192.

Hsü, K.J., LaBrecque, J.L., Carman, M.F., Jr., et al., 1984, Site 524, *in* Hsü, K.J., LaBrecque, J.L., et al., eds., Initial Reports of the Deep Sea Drilling Project, v. 73: Washington, U.S. Government Printing Office, p. 323–386.

Krasheninnikov, V.A., 1973. Cretaceous benthonic foraminifera, Leg 20, Deep Sea Drilling Project, *in* Heezen, B.C., MacGregor, I.D., et al., Initial Reports of the Deep Sea Drilling Project, v. 20: Washington, U.S. Government Printing Office, p. 205–219.

Kroon, D., Norris, R.D., Klaus, A., et al., 1998a, Site 1049, *in* Norris, R.D., Kroon, D., Klaus, A., et al., eds., Proceedings of the Ocean Drilling Program, Initial Reports, v. 171B: College Station, TX (Ocean Drilling Program), 47–91.

Kroon, D., Norris, R.D., Klaus, A., et al., 1998b, Site 1050, *in* Norris, R.D., Kroon, D., Klaus, A., et al., eds., Proceedings of the Ocean Drilling Program, Initial Reports, v. 171B: College Station, TX (Ocean Drilling Program), 93–170.

Lancelot, Y.P., Seibold, E., Čepek, P., et al., 1977, Site 367: Cape Verde Basin, *in* Lancelot, Y.P., Seibold, E., et al., eds., Initial Reports of the Deep Sea Drilling Project, v. 41: Washington, U.S. Government Printing Office, p. 163–232.

Lancelot, Y.P., Larson, R., Fisher, A., et al., 1990, Site 801, *in* Lancelot, Y.P., Larson, R., et al., eds., Proceedings of the Ocean Drilling Project, Initial Reports, v. 129: College Station TX (Ocean Drilling Program), p. 303–416.

Larson, R.L., Moberly, R., Bukry, D., et al., 1975a, Site 310: Hess Rise, *in* Larson, R.L., Moberly, R., et al., eds., Initial Reports of the Deep Sea Drilling Project, v. 32: Washington, U.S. Government Printing Office, p. 295–310.

Larson, R.L., Moberly, R., Bukry, D., et al., 1975b, Site 313: Mid-Pacific Mountains, *in* Larson, R.L., Moberly, R., et al., eds., Initial Reports of the Deep Sea Drilling Project, v. 33: Washington, U.S. Government Printing Office, p. 313–390.

Ludwig, W.J., Krasheninnikov, V.A., Basov, I.A., et al., 1983, Site 511. *in* Ludwig, W.J., Krasheninnikov, V.A., et al., eds., Initial Reports of the Deep Sea Drilling Project, v. 71: Washington, U.S. Government Printing Office, p. 21–110.

Mahoney, J.J., Fitton, J.G., Wallace, P.J., et al., 2001, Leg 192 summary, *in* Mahoney, J.J., Fitton, J.G., Wallace, P.J., et al., eds., Proceedings of the Ocean Drilling Project, Initial Reports, v. 192: College Station TX (Ocean Drilling Program), p. 1–75.

Maxwell, A.E., Von Herzen, R.P., Andrews, J.E., et al., 1970a, Site 20, *in* Maxwell, A.E., Von Herzen, R.P., et al., eds., Initial Reports of the Deep Sea Drilling Project, v. 3: Washington, U.S. Government Printing Office, p. 319–366.

Maxwell, A.E., Von Herzen, R.P., Andrews, J.E., et al., 1970b, Site 21, *in* Maxwell, A.E., Von Herzen, R.P., et al., eds., Initial Reports of the Deep Sea Drilling Project, v. 3: Washington, U.S. Government Printing Office, p. 367–412.

Montadert, L., Roberts, D.G., Auffret, G.A., et al., 1979a, Sites 399, 400, and hole 440A, *in* Montadert, L., Roberts, D.G., eds., Initial Reports of the Deep Sea Drilling Project, v. 48: Washington, U.S. Government Printing Office, p. 35–72.

Montadert, L., Roberts, D.G., Auffret, G.A., et al., 1979b, Site 401, *in* Montadert, L., Roberts, D.G., eds., Initial Reports of the Deep Sea Drilling Project, v. 48: Washington, U.S. Government Printing Office, p. 73–124.

Moore, T.C., Jr., Rabinowitz, P.D., Boersma, A., et al., 1984a, Site 525, *in* Moore, T.C., Jr., Rabinowitz, P.D., et al., eds., Initial Reports of the Deep Sea Drilling Project, v. 74: Washington, U.S. Government Printing Office, p. 41–160.

Moore, T.C., Jr., Rabinowitz, P.D., Boersma, A., et al., 1984b, Site 527, *in* Moore, T.C., Jr., Rabinowitz, P.D., et al., eds., Initial Reports of the Deep Sea Drilling Project, v. 74: Washington, U.S. Government Printing Office, p. 237–306.

Moore, T.C., Jr., Rabinowitz, P.D., Boersma, A., et al., 1984c, Site 528, *in* Moore, T.C., Jr., Rabinowitz, P.D., et al., eds., Initial Reports of the Deep Sea Drilling Project, v. 74: Washington, U.S. Government Printing Office, p. 307–406.

Perch-Nielsen, K., Supko, P.R., Boersma, A., et al., 1977a, Site 354, *in* Supko, P.R., Perch-Nielsen, K., et al., eds., Initial Reports of the Deep Sea Drilling Project, v. 39: Washington, U.S. Government Printing Office, p. 45–100.

Perch-Nielsen, K., Supko, P.R., Boersma, A., et al., 1977b, Site 355, *in* Supko, P.R., Perch-Nielsen, K., et al., eds., Initial Reports of the Deep Sea Drilling Project, v. 39: Washington, U.S. Government Printing Office, p. 101–140.

Perch-Nielsen, K., Supko, P.R., Boersma, A., et al., 1977c, Site 356, *in* Supko, P.R., Perch-Nielsen, K., et al., eds., Initial Reports of the Deep Sea Drilling Project, v. 39: Washington, U.S. Government Printing Office, p. 141–230.

Perch-Nielsen, K., Supko, P.R., Boersma, A., et al., 1977d, Site 357, *in* Supko, P.R., Perch-Nielsen, K., et al., eds., Initial Reports of the Deep Sea Drilling Project, v. 39: Washington, U.S. Government Printing Office, p. 231–328.

Perch-Nielsen, K., Supko, P.R., Boersma, A., et al., 1977e, Site 358, *in* Supko, P.R., Perch-Nielsen, K., et al., eds., Initial Reports of the Deep Sea Drilling Project, v. 39: Washington, U.S. Government Printing Office, p. 329–372.

Peterson, M.N.A., Edgar, N.T., Borch, C. von der, et al., 1970, Site 9, *in* Peterson, M.N.A., Edgar, N.T., et al., eds., Initial Reports of the Deep Sea Drilling Project, v. 2: Washington, U.S. Government Printing Office, p. 35–116.

Quilty, P.G., 1992, Upper Cretaceous planktonic foraminifers and biostratigraphy, Leg 120, southern Kerguelen Plateau, *in* Wise, S.W., Jr., Schlich, R., et al., Proceedings of the Ocean Drilling Program, Initial Reports, v. 120: College Station, TX (Ocean Drilling Program), p. 371–392.

Ryan, W.B.F., Sibuet, J.-C.,. Arthur, M.A., et al., 1979, Site 398, *in* Sibuet, J.-C., Ryan, W.B.F., et al., eds., Initial Reports of the Deep Sea Drilling Project, v. 47, part 2: Washington, U.S. Government Printing Office, p. 25–234.

Schlanger, S.O., Jackson, E.D., Boyce, R.E., et al., 1976a, Site 315, *in* Schlanger, S.O., Jackson, E.D., et al., eds., Initial Reports of the Deep Sea Drilling Project, v. 33: Washington, U.S. Government Printing Office, p. 37–104.

Schlanger, S.O., Jackson, E.D., Boyce, R.E., et al., 1976b, Site 316, *in* Schlanger, S.O., Jackson, E.D., et al., eds., Initial Reports of the Deep Sea Drilling Project, v. 33: Washington, U.S. Government Printing Office, p. 105–160.

Scheibnerova, V., 1974. Aptian–Albian benthonic foraminifera from DSDP Leg 27, Sites 259, 260 and 263, Eastern Indian Ocean, *in* Veevers, J.J., Heirtzler, J.R., et al., Initial Reports of the Deep Sea Drilling Project, v. 27: Washington (U.S. Government Printing Office), p. 697–741.

Scholl, D.W., Boyce, R.E., Echols, R.J., et al., 1973, Site 192, *in* Creager, J.S., Scholl, D.W., et al., eds., Initial Reports of the Deep Sea Drilling Project, v. 19: Washington, U.S. Government Printing Office, p. 463–554.

Sheridan R.E., Gradstein F.M., Barnard, L.A., et al., 1983, Site 534, *in* Sheridan R.E., Gradstein F.M., et al., eds., Initial Reports of the Deep Sea Drilling Project, v. 76: Washington, U.S. Government Printing Office, p. 141–340.

Simpson, E.S.W., Gieskes, J., Girdley, W.A., et al., 1974, Site 249, *in* Simpson, E.S.W., Schlich, R., et al., eds., Initial Reports of the Deep Sea Drilling Project, v. 25: Washington, U.S. Government Printing Office, p. 287–348.

Sliter, V. W., 1977. Cretaceous foraminifers from the Southern Atlantic Ocean, Leg 36, DSDP, *in* Barker, P.F., Dalziel, I.W.D., et al., Initial Reports of the Deep Sea Drilling Project, v. 36: Washington, U.S. Government Printing Office, p. 519–573.

Thiede, J., Vallier, T.L., Adeseck, C. Jr., et al., 1981a, Site 463: Western Mid-Pacific Mountains, *in* Thiede, J., Vallier, T.L., et al., eds., Initial Reports of the Deep Sea Drilling Project, v. 62: Washington, U.S. Government Printing Office, p. 33–156.

Thiede, J., Vallier, T.L., Adeseck, C. Jr., et al., 1981b, Site 464: Northern Hess Rise, *in* Thiede, J., Vallier, T.L., et al., eds., Initial Reports of the Deep Sea Drilling Project, v. 62: Washington, U.S. Government Printing Office, p. 157–198.

Tucholke, B.E., Vogt, P.R., Dermars, K.R., et al., 1979a, Site 382: Nashville Seamount—volcanism along the Eastern New England Seamount Chain, *in* Tucholke, B.E., Vogt, P.R., et al., eds., Initial Reports of the Deep Sea Drilling Project, v. 43: Washington, U.S. Government Printing Office, p. 31–94.

Tucholke, B.E., Vogt, P.R., Dermars, K.R., et al., 1979b, Site 384: The Cretaceous/Tertiary boundary, Aptian reefs, and the J-anomaly Ridge, *in* Tucholke, B.E., Vogt, P.R., et al., eds., Initial Reports of the Deep Sea Drilling Project, v. 43: Washington, U.S. Government Printing Office, p. 107–154.

Tucholke, B.E., Vogt, P.R., Dermars, K.R., et al., 1979c, Site 385: Volcanism at Vogel seamount in the Central New England Seamount Chain, *in* Tucholke, B.E., Vogt, P.R., et al., eds., Initial Reports of the Deep Sea Drilling Project, v. 43: Washington, U.S. Government Printing Office, p. 155–194.

Tucholke, B.E., Vogt, P.R., Dermars, K.R., et al., 1979d, Site 386: Fracture valley sedimentation in the central Bermuda Rise, *in* Tucholke, B.E., Vogt, P.R., et al., eds., Initial Reports of the Deep Sea Drilling Project, v. 43: Washington, U.S. Government Printing Office, p. 195–322.

Tucholke, B.E., Vogt, P.R., Dermars, K.R., et al., 1979e, Site 387: Cretaceous to recent sedimentary evolution of the western Bermuda Rise, *in* Tucholke, B.E., Vogt, P.R., et al., eds., Initial Reports of the Deep Sea Drilling Project, v. 43: Washington, U.S. Government Printing Office, p. 323–392.

Van Andel, T.H., Heath, G.R., Benntee, R.H., et al., 1973, Site 163, *in* Van Andel, T.H., Heath, G.R., Benntee, R.H., et al., eds., Initial Reports of the Deep Sea Drilling Project, v. 16: Washington: U.S. Government Printing Office, p. 411–472.

van Hinte, J.E., Wise, S.W., Biart, B.N.M., et al., 1987, Site 603, *in* van Hinte, J.E., Wise, S.W., et al., eds., Initial Reports of the Deep Sea Drilling Project, v. 93, Part 2: Washington, U.S. Government Printing Office, p. 25–276.

Whitmarsh, R.B., Beslier, M.-O., Wallace, P.J., et al., 1998, Site 1070, *in* Whitmarsh, R.B., Beslier, M.-O., Wallace, P.J., et al., eds., Proceedings of the Ocean Drilling Program, Initial Reports, v. 173: College Station, TX (Ocean Drilling Program), p. 265–296

Winterer, E.L., Ewing, J.I., Douglas, R.G., et al., 1973a, Site 164, *in* Winterer, E.L., Ewing, J.I., et al., eds., Initial Reports of the Deep Sea Drilling Project, v. 17: Washington, U.S. Government Printing Office, p. 17–46.

Winterer, E.L., Ewing, J.I., Douglas, R.G., et al., 1973b, Site 167, *in* Winterer, E.L., Ewing, J.I., et al., eds., Initial Reports of the Deep Sea Drilling Project, v. 17: Washington: U.S. Government Printing Office, p. 145–234.

Winterer, E.L., Ewing, J.I., Douglas, R.G., et al., 1973c, Site 169, *in* Winterer, E.L., Ewing, J.I., et al., eds., Initial Reports of the Deep Sea Drilling Project, v. 17: Washington: U.S. Government Printing Office, p. 247–262.

Winterer, E.L., Ewing, J.I., Douglas, R.G., et al., 1973d, Site 170, *in* Winterer, E.L., Ewing, J.I., et al., eds., Initial Reports of the Deep Sea Drilling Project, v. 17: Washington: U.S. Government Printing Office, p. 263–282.

Worzel, J.L., Bryant, W., Arthur O.B., et al., 1973a, Site 86, *in* Worzel, J.L., Bryant W., et al., eds., Initial Reports of the Deep Sea Drilling Project, v. 10: Washington: U.S. Government Printing Office, p. 1–748.

Worzel, J. L., Bryant, W., Arthur O.B., et al., 1973b, Site 95, *in* Worzel, J.L., Bryant W., et al., eds., Initial Reports of the Deep Sea Drilling Project, v. 10: Washington, U.S. Government Printing Office, p. 1–748.

Zachos, J.C., Kroon, D., Blum, P., et al., 2004. Leg 208 summary, *in* Zachos, J.C., Kroon, D., Blum, P., et al., eds., Proceedings of the Ocean Drilling Project, Initial Reports, v. 208: College Station TX (Ocean Drilling Program), p. 1–112.